https://doi.org/10.1093/plphys/kiac564 PLANT PHYSIOLOGY 2022: 1–20

Plant Physiology®

Research Article

Living with high potassium: Balance between nutrient acquisition and K-induced salt stress signaling

Pramod Pantha [1], Dong-Ha Oh [1], David Longstreth [1] and Maheshi Dassanayake [1,*]

1 Department of Biological Sciences, Louisiana State University, Baton Rouge, Louisiana 70803, USA

*Author for correspondence: maheshid@lsu.edu (M.D.)
The author responsible for distribution of materials integral to the findings presented in this article in accordance with the policy described in the Instructions for Authors (https://academic.oup.com/plphys/pages/General-Instructions) is Maheshi Dassanayake.

Abstract

High potassium (K) in the growth medium induces salinity stress in plants. However, the molecular mechanisms underlying plant responses to K-induced salt stress are virtually unknown. We examined Arabidopsis (*Arabidopsis thaliana*) and its extremophyte relative *Schrenkiella parvula* using a comparative multiomics approach to identify cellular processes affected by excess K and understand which deterministic regulatory pathways are active to avoid tissue damages while sustaining growth. Arabidopsis showed limited capacity to curb excess K accumulation and prevent nutrient depletion, contrasting to *S. parvula* which could limit excess K accumulation without restricting nutrient uptake. A targeted transcriptomic response in *S. parvula* promoted nitrogen uptake along with other key nutrients followed by uninterrupted N assimilation into primary metabolites during excess K-stress. This resulted in larger antioxidant and osmolyte pools and corresponded with sustained growth in *S. parvula*. Antithetically, Arabidopsis showed increased reactive oxygen species levels, reduced photosynthesis, and transcriptional responses indicative of a poor balance between stress signaling, subsequently leading to growth limitations. Our results indicate that the ability to regulate independent nutrient uptake and a coordinated transcriptomic response to avoid non-specific stress signaling are two main deterministic steps toward building stress resilience to excess K^+-induced salt stress.

Introduction

Can excess potassium (K^+) in soil be too much of a good thing for plants? Its role as an essential macronutrient for plants is well established (Wang and Wu, 2013). Because of the known plant growth promoting effects of K when supplemented in agricultural fields, majority of past studies have focused on K^+ uptake into plants from low concentrations in the soil. Soil salinity is defined as the soluble salt content in soil composed of a combination of Na^+, K^+, and other ions (Raza et al., 2022) contrary to the majority of genetic studies exploring salinity stress on plants exclusively using Na^+. Consequently, we barely understand excess K^+-induced salt stress in plants. Additionally, toxicity in plants exposed to high concentrations of plant nutrients such as boron (Wang et al., 2021), copper (Lequeux et al., 2010), and nitrogen (Yoshitake et al., 2021) have been investigated, while the systematic evaluation of molecular phenotypes and associated mechanisms behind K^+ toxicity are less studied.

Worldwide there are many soils naturally high in K^+ leading to saline soils (Kresge et al., 1988; Duval et al., 2005; Warren, 2016). Eighty-five percent of salt-affected top soils are categorized as agriculturally unfavorable saline soils due to a combination of salts including sodium- and K-salts while only the remaining 15% are categorized as sodic soils enriched specifically in Na^+ (FAO, 2021, 2022). Potassium is the seventh most abundant element in the continental crust and weathering of K-containing minerals is one of the major sources of high K^+ in soils followed by excess application of fertilizer (Jobbágy and Jackson, 2001; David, 2010). The use

Received September 28, 2022. Accepted December 07, 2022

of recycled water in agriculture is another indirect anthropogenic cause resulting in extremely high K^+ levels in top soils. Many industrial and agricultural processing plants produce wastewater with exceptionally high K^+ concentrations (Arienzo et al., 2009). During wastewater treatments, unlike N, P, or organic matter which are typically processed using microbial activity, K does not get reduced but rather gets concentrated due to evaporation. This often leads to K^+ levels exceeding 100–1,000-fold compared to nutrient levels optimal for plant growth (Arienzo et al., 2009). The need to use currently abandoned or low yielding agricultural lands due to salinity and recycled wastewater for irrigation due to freshwater scarcity is imperative (IPCC, 2021). These needs cannot be addressed without foundational knowledge on how plant nutrient balance is achieved in the absence of prime agricultural land. Therefore, knowing the tolerance mechanisms against high K becomes an impending need in our quest to convert marginal lands into productive agricultural lands.

Past studies have reported that excess K^+ severely affect growth of multiple crops and even halophytes (Eijk, 1939; Ashby and Beadle, 1957; Eshel, 1985; Matoh et al., 1986; Wang et al., 2001; Ramos et al., 2004; Richter et al., 2019; Zhao et al., 2020). These studies suggest that K^+ may not elicit the same physiological or metabolic stresses Na^+ does and plants may require distinct genetic pathways in addition to canonical salt response pathways (Pantha and Dassanayake, 2020) to survive high K-induced salt stress.

In this study, we aimed to identify K-induced salt stress responses and deduce the underlying cellular mechanisms plants have evolved to adapt to K-toxicity. We compared Arabidopsis (*Arabidopsis thaliana*), sensitive to high K^+, to its extremophyte relative, *Schrenkiella parvula* that thrives in high K^+ soils (Nilhan et al., 2008; Oh et al., 2014). We examined stress responses exhibited by the two model species to high K^+ treatments using a multiomics approach (Supplemental Figure 1) to identify the relevant genetic pathways influential in regulating or are affected by K-toxicity. Our results revealed an extensive ionomic, metabolic, and transcriptomic reprogramming during high K stress in the stress-sensitive model while providing insights into how the extremophyte model had evolved alternative metabolic and transcriptomic adjustments to enable growth under excess K.

Results

KCl is more toxic than NaCl at the same osmotic strengths

Excess K^+ exerted more severe growth disturbances than observed for Na^+ at the same concentrations in both species (Figure 1; Supplemental Figures 2 and 3). The extremophyte, *S. parvula*, was more resilient to higher concentrations of KCl than Arabidopsis before it showed significant alterations to root, leaf, or silique development (Figure 1, B–D; Supplemental Figures 2 and 3). CO_2 assimilation was reduced in Arabidopsis in response to 150 mM KCl within 24 hours after treatment (HAT), corresponding to a reduction in total shoot carbon (Figure 1, E and F). Under long-term treatments, there was a greater reduction in total leaf area in both species with excess K^+ than Na^+ compared to control conditions (Figure 1D). These results suggest that despite similar levels of osmotic stress elicited by K^+ and Na^+ at equal concentrations, K^+ may exert additional stresses different from Na^+ that may initiate unique responses.

To eliminate the possibility that plant toxicity effects at 150 mM KCl treatments were caused by excess K^+, and not by excess Cl^-, we further treated both species with different K-salts (KNO_3 and K_2SO_4) that presented similar osmotic strengths with constant [K^+]. In Arabidopsis both primary root length and lateral root number consistently significantly decreased compared to control conditions under high K^+ despite the anion used for the salt treatments (Supplemental Figure 4). Our results are consistent with the observations Zhao et al., 2020 reported for Arabidopsis grown under 100 mM K^+ and Na^+ salts given with Cl^- or SO_4^{2-} to deduce that K was more toxic compared to Na^+ and Cl^- at comparable concentrations.

Overall, 150 mM KCl was sufficient to induce physiological stress responses in Arabidopsis within a 3-day period, while impacting long-term growth in *S. parvula*. Notably, KCl treatments at 200 mM KCl given for 2 weeks were lethal to Arabidopsis in tested conditions (Figure 1G). Fresh weight of Arabidopsis plants grown hydroponically for 28 days significantly decreased within 24 h of 150 mM KCl treatment albeit no significant change in dry weights in either species (Supplemental Figure 2B). Therefore, we wanted to ensure that this treatment duration and intensity did not cause excessive internal cell death in Arabidopsis roots, although Arabidopsis did survive long-term 150 mM KCl treatments. We assessed cell viability in treated plants using propidium iodide (Supplemental Figure 5). We observed intact cells and root tissue with new root hair and lateral root development indicative of actively growing roots in the absence of excessive cell death up to 72 h of exposure to 150 mM KCl. Therefore, we selected 150 mM KCl for our cross-species comparative-omics study to investigate K^+ toxicity responses, when both species are expected to show active cellular responses during the early stages of the treatment at 0, 3, 24, and 72 HAT (Supplemental Figure 1).

Excess K^+ causes nutrient depletion in Arabidopsis but not in *S. parvula*

Plants have evolved multiple transporters to facilitate K^+ entry into roots rather than its exit pathways (Shabala and Cuin, 2008). Therefore, we hypothesized that high K^+ in soils will lead to high K^+ contents in plants and that shoots will accumulate more of the excess K^+ in the transport sequence of soil–root–shoot. We predicted that the differential tissue compartmentalization of K^+ will alter K-dependent cellular

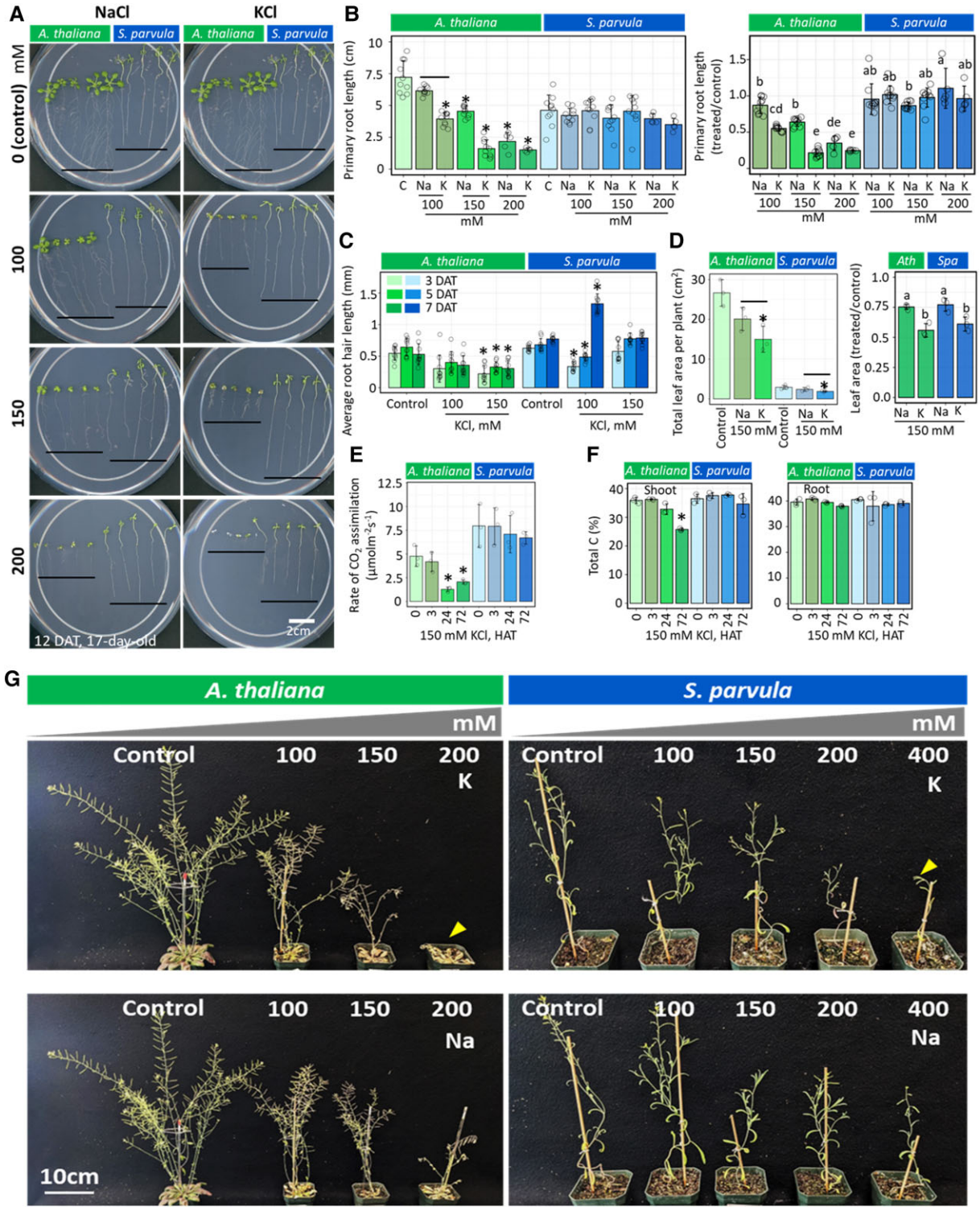

Figure 1 KCl is more toxic than NaCl at the same osmotic strength. A, Seedlings of *Arabidopsis thaliana* (Ath; on the left for each plate) and *S. parvula* (Spa; on the right for each plate) on 1/4 MS media supplemented with 0 (control) to 200 mM NaCl and KCl. Black line on plates refers to the end of the root growth. The control plates for NaCl and KCl are same. B, Primary root length measured on 17-day-old seedlings grown under conditions used in (A) based on a 12-day treatment of NaCl or KCl. C, Average root hair length (average length taken from 10 longest root hairs) measured under the same growth conditions used in [a] for variable KCl treatments and monitored for a week. D, Leaf area measured for hydroponically grown Arabidopsis and *S. parvula* treated with increasing levels of NaCl and KCl until the appearance of first flower. E, Photosynthesis measured as the rate of CO_2 assimilation of the entire shoot/rosette in 25-day-old hydroponically grown plants and monitored up to 72 HAT. F, Total carbon as a % weight based on total dry mass for root and shoot tissue under conditions used in (E). G, 21-day-old plants treated

(continued)

processes. With elemental profiling of 18 nutrients and six common toxic elements (Supplemental Methods, Supplemental Figure 1, Supplemental Table 1), we aimed to test if high K^+ would (1) accumulate as an isolated process; (2) cause nutrient imbalances; or (3) allow entry of other toxic elements and thereby indirectly cause toxicity symptoms.

Shoot K^+ levels were higher than levels in roots, but this difference was strikingly larger in *S. parvula* than in Arabidopsis under control conditions (Figure 2A). Importantly, *S. parvula* maintained shoot K^+ levels comparable to its control during K^+ treatments (Figure 2A). The total K content in whole plants was significantly higher at 72 HAT for both species although we observed there were species-specific differences in root and shoot K distributions that were time-dependent (Figure 2A; Supplemental Figure 6A).

Potassium accumulation in Arabidopsis resulted in a severe nutrient imbalance leading to the depletion of seven nutrients including nitrogen (N; Figure 2, B–D). The depletion of total N in Arabidopsis was further detected as a total decrease in the NO_3^- content (Supplemental Figure 6B). In line with uninterrupted root growth observed under 150 mM KCl (Figure 1, A–C), *S. parvula* showed a remarkable capacity in maintaining its macronutrients levels (Figure 2D). Moreover, other elements did not accumulate under excess K^+ to suggest indirect toxicity effects in either species (Figure 2C). The overall ionomic profiles suggest that constraining K^+ accumulation while upholding other nutrient uptake processes is necessary for K^+ toxicity tolerance.

S. parvula is more responsive than Arabidopsis at the metabolome level to excess K^+ stress

We obtained 472 (145 known and 327 unannotated) metabolite profiles across tissues and time points to identify metabolic processes influenced by K^+ stress (Supplemental Table 2). The relative abundances of metabolites were highly correlated between the two species for similar conditions (Figure 3A). For downstream analysis, we only considered the known metabolites with significant abundance changes (MACs) between control and KCl treated conditions (Figure 3B).

We observed three distinct trends from metabolite profile comparisons (Figure 3, B–D). First, with longer stress durations, the number of MACs increased in both species. Second, *S. parvula* contained more MACs in roots, even though it had fewer physiological and ionomic adjustments compared to Arabidopsis under excess K^+ (Figures 1 and 2). Arabidopsis shoots had more MACs than in *S. parvula* consistent with a reduction in photosynthesis seen in Arabidopsis during K^+ toxicity (Figure 1C). Third, more MACs in *S. parvula* increased in abundances contrasting to the depletion of those in Arabidopsis (Figure 3D). Amino acids were dominant among *S. parvula* MACs compared to sugars dominant among Arabidopsis MACs (Figure 3D). Our results suggest that the two species use two distinct primary metabolite groups to respond to excess K^+ in addition to contrasting shoot-root responses in line with having only a few MACs under shared responses between the species (Figure 3B).

We predicted that *S. parvula* was enriched in MACs that minimized cellular stress, while MACs in Arabidopsis were more representative of pathways disrupted by K^+ toxicity. Galactose metabolism was significantly enriched among MACs in *S. parvula* roots and Arabidopsis shoots (Supplemental Figure 7A). Galactose metabolism includes several key metabolites (Supplemental Figure 7B) known to protect plants against oxidative and osmotic stresses (Taji et al., 2002; Nishizawa et al., 2008). Interestingly, these increased uniquely in *S. parvula* roots (Supplemental Figure 7B). Antioxidants and osmoprotectants (galactinol, raffinose, myo-inositol, sucrose, and proline; Taji et al., 2002; Gong et al., 2005; Nishizawa et al., 2008) increased in *S. parvula* compared to Arabidopsis (Figure 3D; Supplemental Figure 7B). Collectively, the extremophyte, *S. parvula*, seemed to boost the protective metabolites minimizing damage from oxidative bursts in its roots, while the more stress sensitive species, Arabidopsis, was depleting its initial pools of such protective metabolites during stress.

Arabidopsis transcriptional responses are inept against K^+ toxicity

We examined the transcriptional response landscapes to deduce distinct cellular processes initiated by Arabidopsis and *S. parvula* upon excess K^+. *S. parvula* showed lesser transcriptome-wide variation than Arabidopsis based on a PCA of 23,281 ortholog pairs (Figure 4A). Transcriptome similarities between tissues were consistent with high correlations between samples within a tissue/species (Supplemental Figure 8). The total number of differentially

Figure 1 (Continued)
for 14 days (salt applied every other day). Imaged 20 days after the completion of the treatment. Arabidopsis plants treated with KCl show more severe salt stress effects compared to the same concentration of NaCl. In Arabidopsis, 200 mM KCl treated plants did not develop any flowers (as indicated by arrowhead) while 200 mM NaCl treated plants flowered and developed siliques. In *S. parvula*, a similar observation was made at 400 mM KCl as indicated by yellow arrowhead. The control plants used in the NaCl and KCl treatment assays were the same for both species. Minimum five plants per condition used in B and a minimum of three plants per condition used for D and E. Asterisks indicate significant changes between the treated samples to its respective control samples (*t* test with $P \leq 0.05$). Same letters in the bar graph indicate that those samples are not significantly different (one-way ANOVA followed by Tukey's post-hoc test, *P*-value ≤ 0.05). Data are presented as a mean of at least three independent biological replicates ± SD. Open circles indicate the measurement from each plant (B,C) and replicate (D–F). DAT, days after treatment; HAT, hours after treatment.

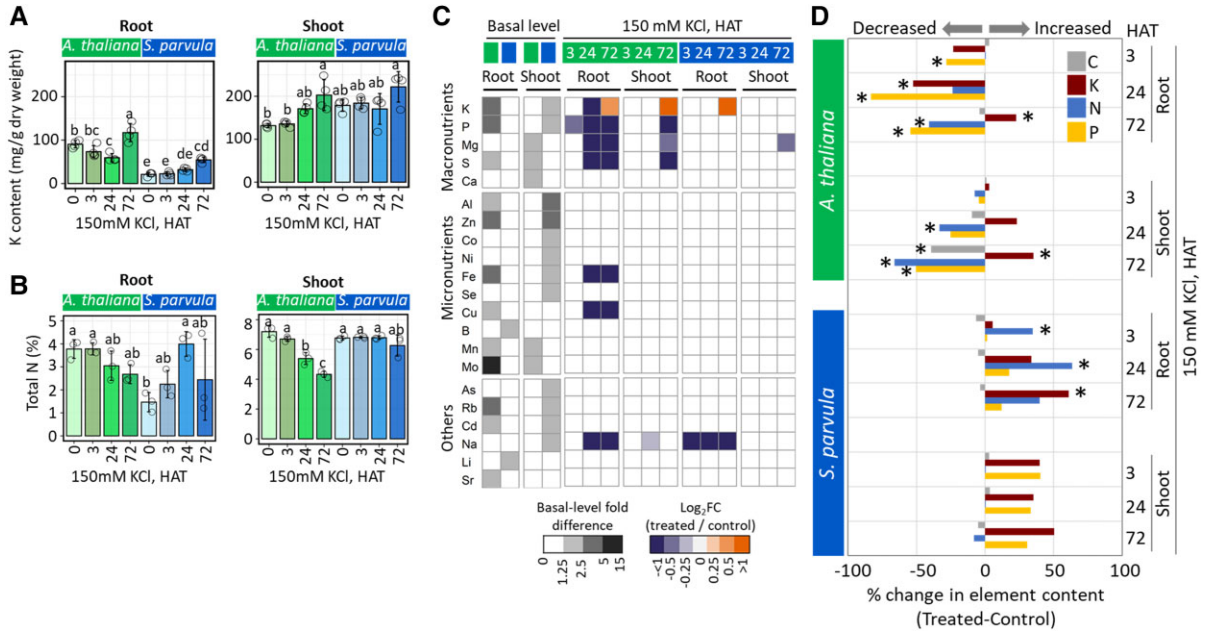

Figure 2 Excess K accumulation caused severe nutrient imbalance in Arabidopsis compared to *S. parvula*. A, K accumulated differently between Arabidopsis and *S. parvula*. Arabidopsis promoted shoot retention while *S. parvula* promoted root retention of K. B, Increased accumulation of K resulted in N depletion in Arabidopsis compared to *S. parvula*. C, Differential accumulation of K caused imbalances of multiple nutrients in Arabidopsis roots even in early time points and caused hardly any noticeable differences in *S. parvula*. D, Percent change in CNPK elemental content in root and shoot of Arabidopsis and *S. parvula* under high [K^+]. Arabidopsis fails to maintain major macronutrient levels preventing depletion of those pools contrasted to *S. parvula*. Data are represented as mean of at least 4 (for A and C) and 3 (for B) independent replicates with ± SD given using ≥ 5–8 hydroponically grown plants per replicate. Elemental compositions were quantified using ICP-MS and total N and C was obtained using an elemental combustion system. Nitrogen and carbon was measured separately but from the same plant samples. The total elemental composition is reported after normalization for dry weight. All quantitative measurements were evaluated by one-way ANOVA followed by Tukey's post-hoc test, *P*-value ≤ 0.05 and same letters in the bar graph does not differ statistically significantly and asterisks indicate significant changes between the treated samples to its respective control samples. Open circles indicate the measurement from each replicate. HAT, hours after treatment.

expressed genes (DEGs) was remarkably higher in Arabidopsis (9,907 in roots and 12,574 in shoots) compared to those in *S. parvula* (1,377 in roots and 494 in shoots) calculated using raw count value (Supplemental Figure 9, Supplemental Tables 3 and 4).

We annotated all DEGs with a representative gene ontology (GO) function (Supplemental Tables 4 and 5) and examined their time-dependent progression in Arabidopsis (Figure 4B; Supplemental Figure 9, Supplemental Tables 6–9). The temporal transcriptomic response was the highest at 24 and 72 HAT in roots and shoots, respectively (Figure 4B). One of the primary emergent functions enriched in Arabidopsis was response to stress (Figure 4B). Within this category, the prevalent specific responses across all-time points were responses to salt, oxidative, and ionic stresses. Biotic stress-related GO terms (e.g. response to bacterium, response to chitin, and immune response) were also prominently enriched at all-time points (Figure 4B) in Arabidopsis, which seemed counterintuitive when *S. parvula* orthologs of those were mostly either unchanged or suppressed (Supplemental Tables 4 and 8). We examined if this was a sign of transcriptional misregulation at the peak response time inept to the extant stress experienced by Arabidopsis.

We observed three indicators to suggest that there was broad misregulation in transcriptional responses upon excess K^+ accumulation in Arabidopsis. First, transcriptional responses were enriched for all major plant hormone pathways in shoots beyond the expected enrichment associated with ABA, suggestive of wide-ranging disruptions to hormone signaling (Figure 4B). Second, we found autophagy as the most enriched process among DEGs, accompanied by additional enriched processes including cell death and leaf senescence. Third, enriched responses to cold, heat, wounding, drought, and hypoxia suggestive of unmitigated oxidative stress were prevalent during 24–72 HAT (Figure 4B). Therefore, we assessed the ROS accumulation in Arabidopsis and *S. parvula* leaves during high K^+ stress using oxidative stress markers, H_2O_2 and O_2^-. As predicted by the transcriptional response, leaves of Arabidopsis showed severe oxidative stress compared to *S. parvula* (Figure 4C). While fewer DEGs at 72 HAT compared to 24 HAT implied a degree of stress acclimation in Arabidopsis (Figure 4B; Supplemental Figure 9), the prolonged ABA signaling together with broad activation of hormone pathways, autophagy, and oxidative stress serve as transcriptional molecular phenotypes to indicate inept responses in Arabidopsis. These molecular

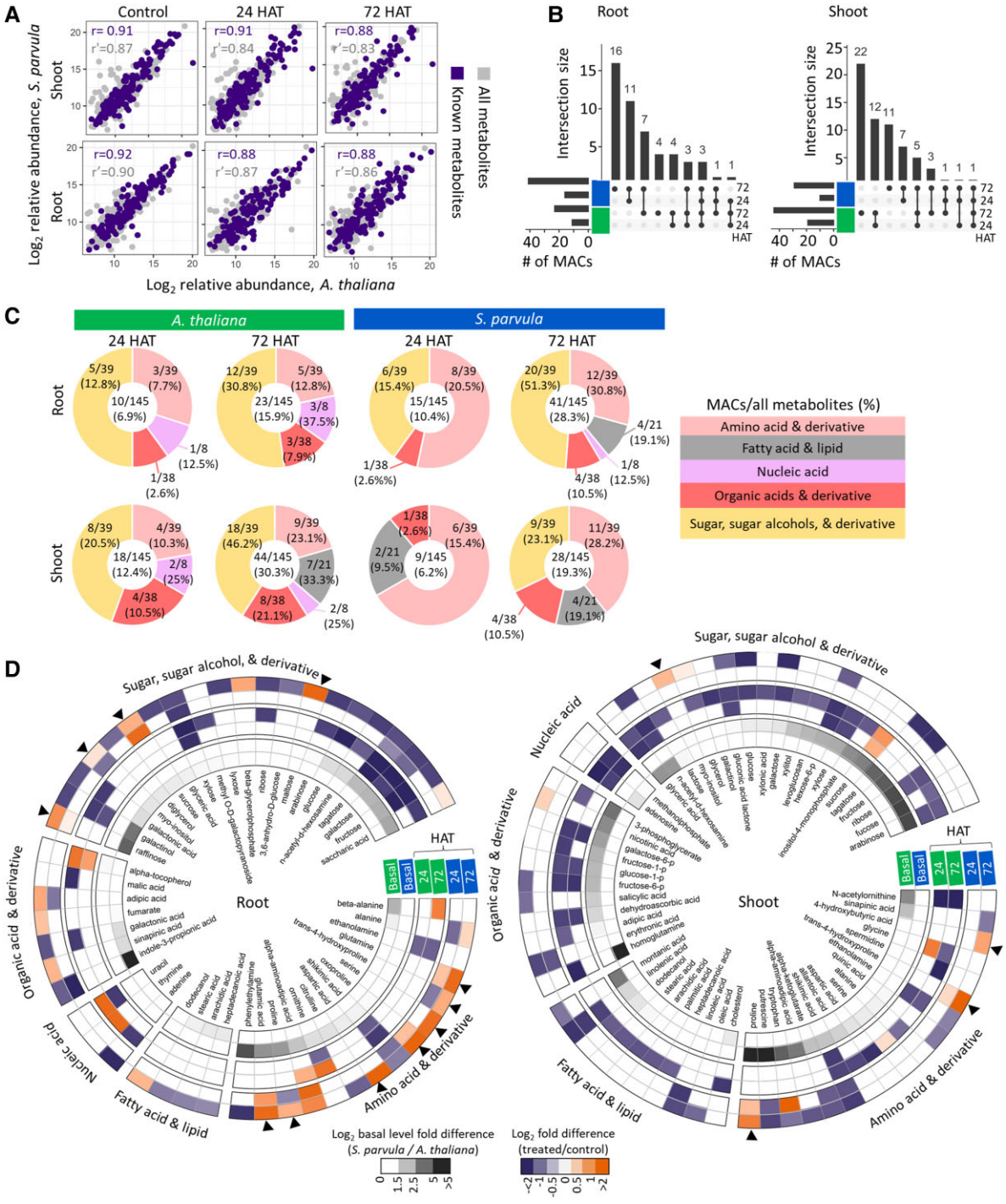

Figure 3 *S. parvula* root metabolome is more responsive than Arabidopsis and induces specific antioxidants and osmoprotectants to adapt to high K^+ stress in both roots and shoots. A, Arabidopsis and *S. parvula* metabolome profiles are highly corelated with each other upon high K^+ in both roots and shoots. Pearson correlation coefficient is calculated for 145 known metabolites (r) and all metabolites including the unannotated metabolites (r'). B, Known metabolites that significantly changed in abundance at 24 and 72 HAT. C, Overview of the temporal changes in primary metabolic pools based on known metabolite annotations. Metabolites that significantly changed in abundance at respective time points are shown followed by a "/" and the total number of metabolites counted in that category. D, Individual metabolites in each functional group mapped to represent their abundance starting at basal level (inner circles) to 24 and 72 h of exposure to high K shown in concentric outer rings. Metabolites mostly highlighted in Results and Discussion are marked with arrow heads in the outer circle in both plots. Significance test for metabolite abundance was performed with one-way ANOVA followed by Tukey's post-hoc test, P-value ≤ 0.05. Data are represented as mean of at least three independent replicates using ≥ 5 hydroponically grown plants per replicate.

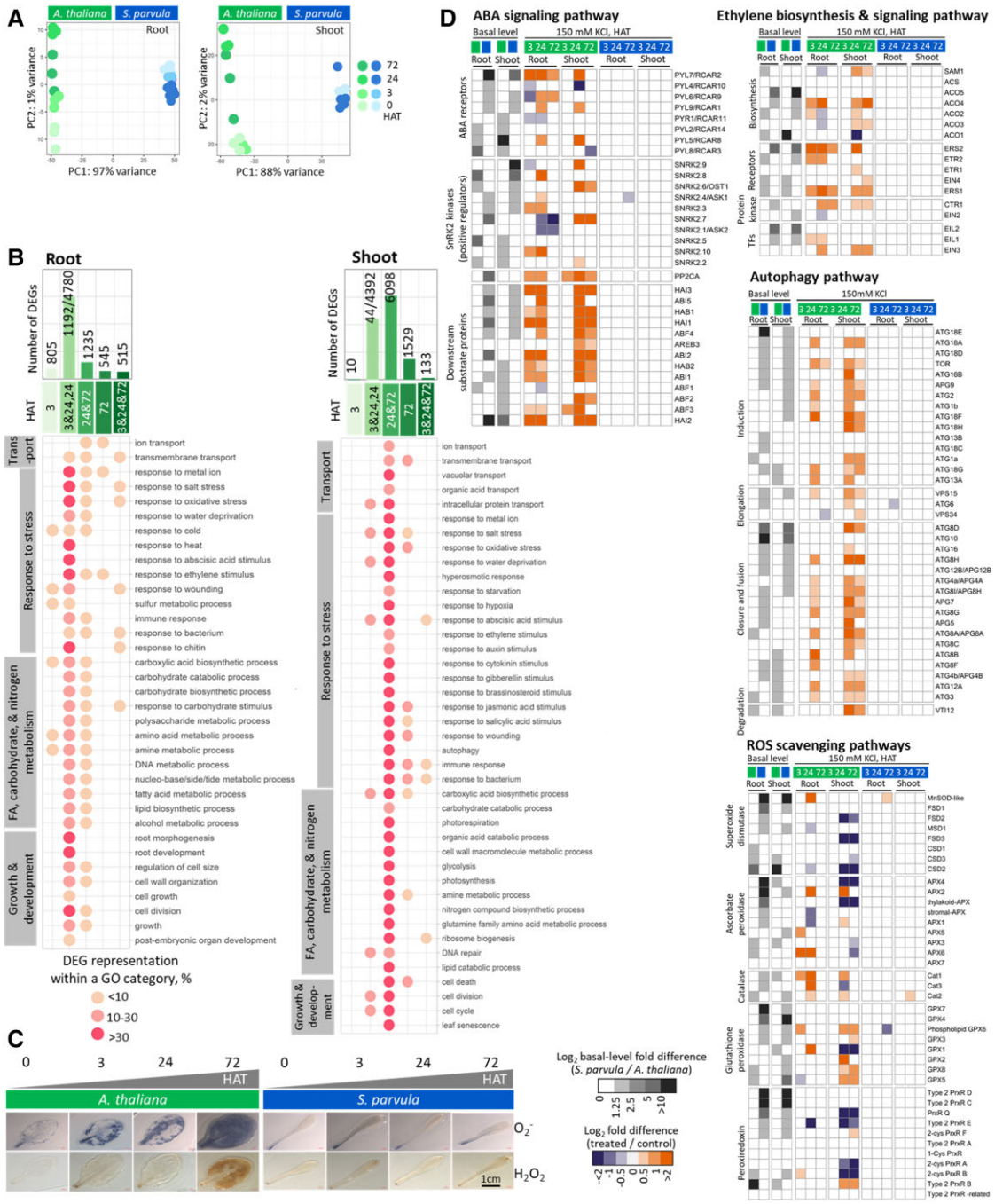

Figure 4 Arabidopsis shows nonselective transcriptional modifications during excess K^+ stress than *S. parvula*. A, Principal component analysis (PCA) of ortholog (23,281 ortholog pairs) expression between Arabidopsis and *S. parvula* root and shoot transcriptomes at 0, 3, 24, and 72 HAT. B, Enriched functional processes based on GO annotations associated with DEGs in Arabidopsis. The temporal sequence of enriched functions is given as 3 h specific, 3 and 24 h together with 24 h specific, 24 and 72 h shared, 72 h specific, and present at all-time points from 3–24–72 h. Only functional processes that were detected at least in two time points are shown and the processes are sorted based on their functional hierarchy when applicable. C, Arabidopsis accumulated higher levels of hydrogen peroxide (H_2O_2) and superoxide ions (O_2^-) in leaves under excess K^+ stress compared to *S. parvula*. Hydroponically grown plants were used treated similar to the plants used for the RNA-seq study and stained with DAB and NBT. D, Transcriptional profiles of selected pathways that serve as indicators of transcriptional mismanagement in Arabidopsis during excess K^+ stress compared to *S. parvula*. DEGs were called using DESeq2 with a *P*-adj. value based on Benjamini–Hochberg correction for multiple testing set to < 0.01. Data are represented as mean of three independent replicates using ≥ 5 hydroponically grown plants per replicate.

phenotypes become even more compelling when compared to their respective orthologous profiles in *S. parvula* which remained mostly unchanged (Figure 4D).

Carboxylic acid/carbohydrate and amino acid metabolism formed the second largest group among the most affected processes following stress responses (Figure 4B). These processes were enriched at all-time points in Arabidopsis roots and shoots consistent with the previous physiological and metabolic responses that showed primary C and N metabolism were severely affected (Figures 1, E and F, 2D, and 3, C and D). Interruptions to photosynthesis at 24 and 72 HAT (Figure 1E) were aligned with the corresponding transcriptional processes enriched at the same time points in Arabidopsis shoots (Figure 4B). Contrarily, root development was detected as a transcriptionally enriched process at 3 HAT (Figure 4B), although the interruptions to root hair growth was detected at 72 HAT (Figure 1C).

S. parvula shows targeted transcriptomic responses steered toward stress tolerance

We searched for DEGs among Arabidopsis whose *S. parvula* orthologs also showed active responses (Figure 5A). We posited that these orthologs represented cellular processes that require active transcriptional adjustments to survive the accumulation of excess K^+. We further predicted that the diametric inter-species transcriptional responses (i.e. genes that are induced in one species when their orthologs are suppressed in the other species) will be deleterious to the stress sensitive species, while shared responses will be beneficial yet likely underdeveloped or unsustainable to survive prolonged stress in the stress sensitive species (Figure 5A; Supplemental Figure 9 and Supplemental Table 10).

Response to stress was the largest functional group representative of diametric responses showing induction in Arabidopsis compared to suppression in *S. parvula* (Supplemental Figure 9). Most of the subprocesses in this cluster were associated with biotic stress (Supplemental Table 10). Therefore, we further assessed this transcriptional divergence between the two species as a proportional effort invested in biotic versus abiotic stress out of total nonredundant DEGs within each species (Figure 5B). The effort to suppress biotic stress in *S. parvula* roots (10%) was similar to the proportional induction for biotic stress in Arabidopsis (9%; Figure 5B). Contrarily, orthologs that were suppressed in Arabidopsis, but induced in *S. parvula* roots were associated with ion transport and cell wall organization (Supplemental Figure 9A). These transcriptional adjustments support the physiological response observed for *S. parvula* where uncompromised root growth was coincident to uninterrupted nutrient uptake during exposure to excess K^+ (Figures 1B and 2C). The orthologs suppressed in Arabidopsis but induced in *S. parvula* shoots were enriched in carboxylic acid and amine metabolism and transport functions (Supplemental Figure 9B). Collectively, the antithetical transcriptomic, metabolic, ionomic, and physiological responses between the two species support the stress-resilient growth of *S. parvula* distinct from Arabidopsis (Figures 1–5).

The orthologs that showed shared inductions (156 in roots and 199 in shoots) were largely represented by abiotic stress responses (Supplemental Figure 9 and Supplemental Table 11). The orthologs with shared suppression (149 in roots and 84 in shoots) were enriched in biotic stress responses in roots and photosynthesis in shoots. However, suppressed orthologs associated with biotic stress in Arabidopsis (0.004%) were minimal based on a proportional effort compared to that in *S. parvula* (10%; Figure 5B).

Over 50% of orthologs differently expressed in response to excess K^+ in *S. parvula* roots and ~30% in shoots showed unique expression trends different from Arabidopsis (Figure 5A). We postulated that *S. parvula* activates decisive transcriptional regulatory circuits that are either absent (i.e. *S. parvula*-specific responses) or organized differently (i.e. diametric responses) than in Arabidopsis when responding to excess K^+ stress.

The overall transcriptomic response of *S. parvula* encapsulates induction of more targeted salt stress responses than that of Arabidopsis, including oxidative stress responses, sugar and amino acid metabolism, and associated ion transport, with concordant induction in growth promoting processes and transcriptional resource recuperation by suppressing biotic stress responses (Figure 5C). The transcriptional effort to facilitate growth amidst excess K^+ accumulation in tissues is reflected by induced transcripts involved in cell wall biogenesis, RNA processing, and development along with concurrent suppression for rapid growth limiting processes such as cell wall thickening and callose deposition (Supplemental Table 11).

Balance between differential expression of genes encoding K^+ transporters

The ability in *S. parvula* to curb K^+ accumulation and prevent the depletion of major nutrients (Figure 2; Supplemental Figure 6) led us to hypothesize that genes encoding ion transporters are differentially expressed to prevent nutrient imbalance during excess K^+ stress. Moreover, ion transport was among the most represented functions within and between species transcriptome comparisons (Figures 4B and 5C; Supplemental Figure 9A). We predicted that the genes coding for transporters which allow K^+ into roots and upload to the xylem or phloem would be primary targets for down-regulation in the effort to restrain K^+ accumulation, while inducing those that aid in vacuolar sequestration.

We first searched for genes that encoded K^+ transporters that showed statistically significantly different basal level abundances (Figure 6A) or/and responses to high K^+ (Figure 6B). We categorized those into four transport routes: (1) limit entry into roots, (2) promote efflux from roots, (3) constrain long-distance transport between root and shoot, and (4) enhance sequestration into vacuoles. We then

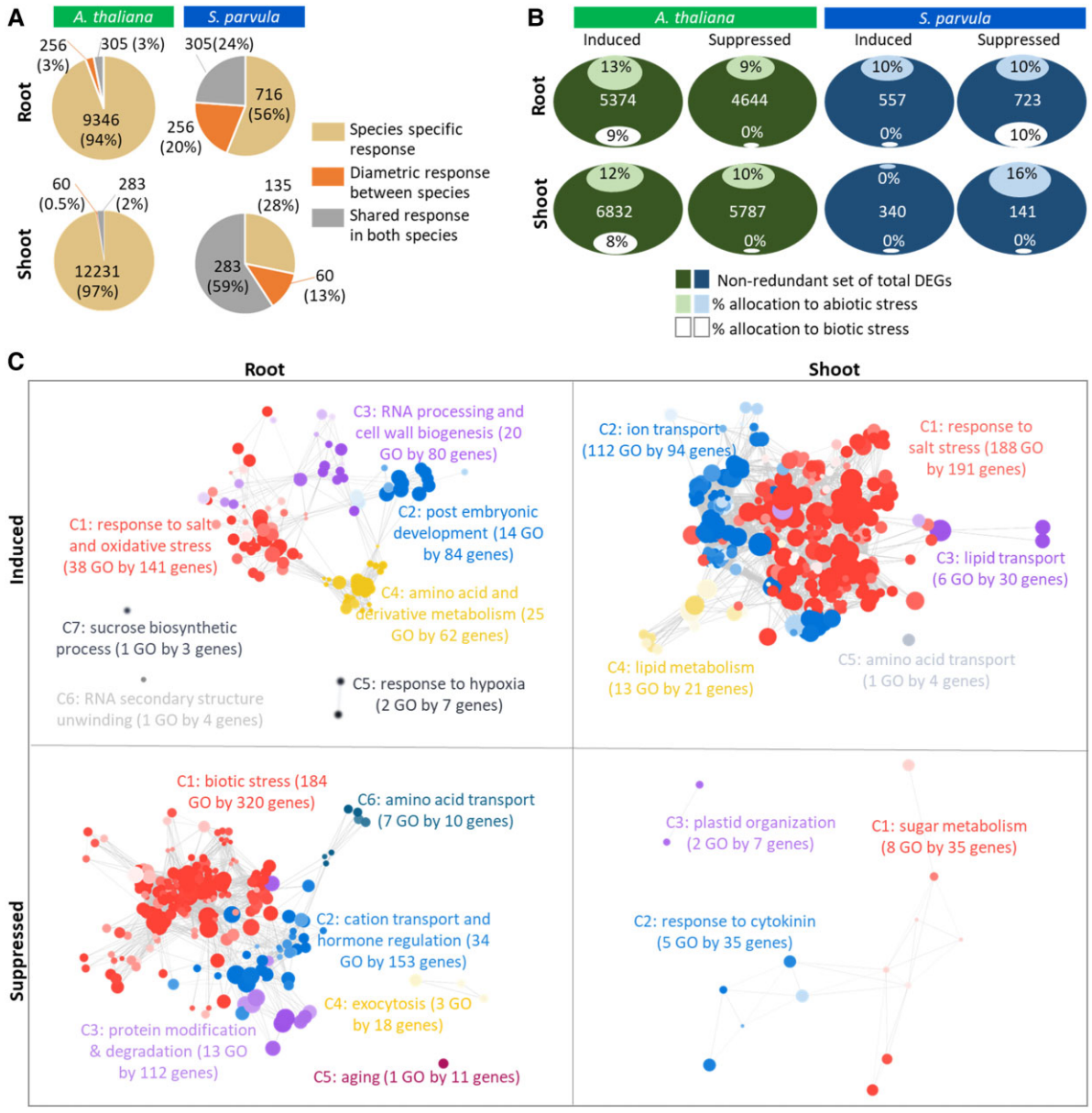

Figure 5 *S. parvula* shows a confined transcriptomic response geared toward concurrent induction of abiotic stress responses and enhanced transcriptional allocation to C and N metabolism. A, The overall expression specificity and response direction of orthologs in Arabidopsis and *S. parvula*. Selected orthologs are DEGs at least in one time point compared to the respective control condition and then counted as a nonredundant set when all 3, 24, and 72 HAT samples were considered for total counts. B, The proportion contributing to abiotic and biotic stress stimuli within nonredundant DEGs. The effort to suppress biotic stress responses in *S. parvula* roots (10%) was similar to the proportional induction for biotic stress responses in Arabidopsis (9%). C, The functionally enriched processes represented by DEGs in *S. parvula* that responded to high K^+. A nonredundant set from all-time points (3, 24, and 72 HAT) are given. A node in each cluster represents a GO term; size of a node represents the number of genes included in that GO term; the clusters that represent similar functions are given a representative cluster name, ID, and also shares the same color; and the edges between nodes show the DEGs that are shared between functions. All clusters included in the network have adj. *P*-values ≤ 0.05 with false discovery rate correction applied. More significant values are represented by darker node colors. The functional enrichment network was created using GOMCL. DEGs were called using DESeq2 with a *P*-adj. value based on Benjamini–Hochberg correction for multiple testing set to < 0.01. Data are represented as mean of three independent replicates using ≥ 5 hydroponically grown plants per replicate.

assessed routes that were potentially weakened in Arabidopsis and/or alternatively regulated in *S. parvula*.

a) *Limit entry into roots*: The most suppressed gene (13-fold reduction) in Arabidopsis under excess K^+ is the *HIGH-AFFINITY K^+ TRANSPORTER 5* (*HAK5*; Gierth et al., 2005), which encodes a major transporter for K^+ uptake during low K^+ availability (Figure 6B). Under sufficient K^+ levels, the low affinity transporter, ARABIDOPSIS K TRANSPORTER 1 (AKT1) with

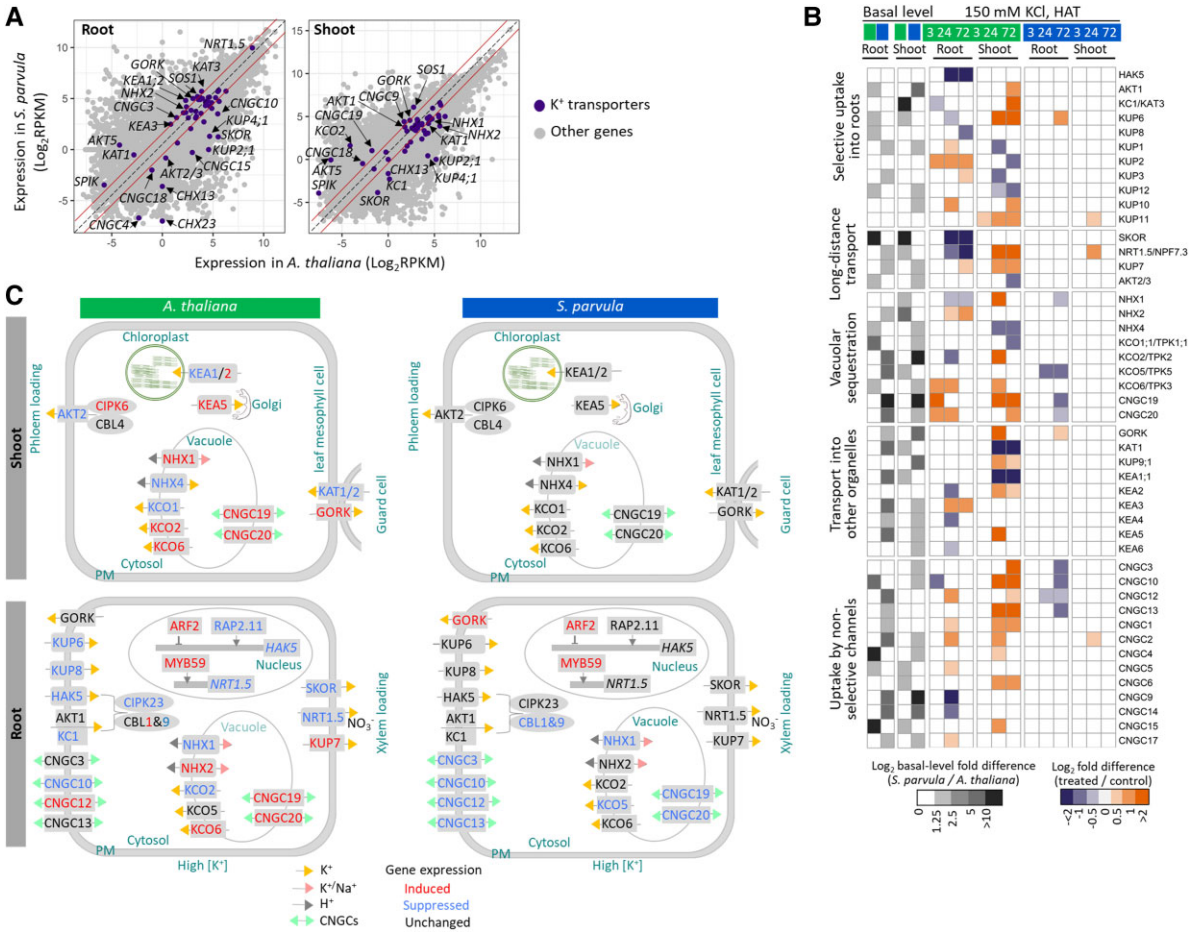

Figure 6 Differential expression of K^+ transporters in Arabidopsis and *S. parvula*. A, Basal level expression comparison of orthologs between Arabidopsis and *S. parvula* in roots and shoots. The dash diagonal line marks identical expression in both species and solid lines represent a two-fold change in one species compared to the other species. Transporters/channels with >two-fold change basal differences between the species are labeled. B, The temporal expression of functionally established K^+ transporters and channels in Arabidopsis and their *S. parvula* orthologs upon high K^+ treatment. C, Key K^+ transporters and channels differently regulated between roots and shoots in Arabidopsis and *S. parvula*. DEGs at each time point were called using DESeq2 compared to 0 h with a *P*-adj. value based on Benjamini–Hochberg correction for multiple testing set to < 0.01. Data are represented as mean of three independent replicates using ≥ 5 hydroponically grown plants per replicate.

POTASSIUM CHANNEL 1 (KC1) is activated (Gierth et al., 2005; Wang et al., 2016). HAK5 and AKT1 are activated by the protein kinase complex, CALCINEURIN B-LIKE PROTEINS 1 and 9 (CBL1&9)/CBL-INTERACTING PROTEIN KINASE 23 (CIPK23; Ragel et al., 2015). Under excess K^+ stress both transporter complexes and their core regulatory unit in Arabidopsis roots were suppressed (Figure 6B and C; Supplemental Figure 10A). Interestingly, the orthologous transporters in *S. parvula* roots were unchanged but the orthologs of the interacting kinase complex were suppressed (Figure 6B; Supplemental Figure 10A). The transcriptional effort to limit entry of K^+ into roots during K^+ stress is further exemplified by the suppression of *RELATED TO AP2 11* (*RAP2.11*), a transcriptional activator of *HAK5* (Kim et al., 2012) and the induction of *AUXIN RESPONSE FACTOR 2* (*ARF2*), a repressor of *HAK5* transcription (Zhao et al., 2016), in Arabidopsis roots (Figure 6C). Similarly, *ARF2* was induced in *S. parvula* roots. Other K^+ transporters associated with K^+ uptake into roots were suppressed in Arabidopsis [e.g. K^+ UPTAKE PERMEASE 6 (KUP6) and KUP8] under excess K^+ stress (Figure 6B). Alternatively, *S. parvula* roots showed a concerted transcriptional suppression of multiple genes encoding cyclic nucleotide gated channels, CYCLIC NUCLEOTIDE GATED CHANNEL 3 (CNGC3)/10/12/13 (Figure 6, B and C). This suggested limitations to nonselective uptake of K^+ into roots (Gobert et al., 2006; Guo et al., 2008).

b) *Promote efflux from roots*: K^+ efflux transporters in plants that exclusively extrude excess K^+ from roots to soil are unknown. In *S. parvula* induced expression levels for *GATED OUTWARDLY-RECTIFYING* K^+

CHANNEL (*GORK*; a K^+ outward rectifying channel; Ivashikina et al., 2001) and *SALT OVERLY SENSITIVE 1* (*SOS1*; Na^+ exporter; Shi et al., 2000) in roots are notable (Figure 6; Supplemental Figure 11). Induction of *GORK* is known to cause K^+ leakage from roots under biotic and abiotic stresses in plants leading to programmed cell death (Demidchik et al., 2014). Arabidopsis did not induce the expression of *GORK* in roots at any of the tested time points. *S. parvula* shows induction of *GORK* in roots without the corresponding transcriptomic signatures for cell death as expected in Arabidopsis (Figures 6, B, C and 4, B–D; Supplemental Figure 6). We also note that the basal expression of *GORK* in *S. parvula* roots is higher than in Arabidopsis roots (Figure 6A; Supplemental Figure 11). SOS1, the antiporter with the highest Na^+ efflux capacity in roots, is known for its Na^+ specificity (Oh et al., 2009). Therefore, induction of *SOS1* in *S. parvula* under high K^+ stress (Supplemental Figure 11) is likely an effort to counterbalance the increasing osmotic stress due to elevated K^+ by exporting available Na^+ from roots. This explanation fits with Na^+ being the only ion depleted in *S. parvula* roots during excess K^+ (Figure 2C).

c) *Constrain long-distance transport between roots and shoots*: The long-distance transport of K^+ via xylem loading is mediated by STELAR K^+ OUTWARD RECTIFIER (SKOR), NITRATE TRANSPORTER 1.5 (NRT1.5), and KUP7 in Arabidopsis (Gaymard et al., 1998; Han et al., 2016; Li et al., 2017). *SKOR* and *NRT1.5* were suppressed in Arabidopsis roots as predicted. However, *KUP7* showed induction in Arabidopsis roots at 72 HAT concordantly when K^+ accumulation was observed in shoots (Figures 2A and 6B). Contrastingly, none of these transporters were differently regulated in *S. parvula* roots. AKT2 is the dominant channel protein regulating long-distance transport via loading and unloading to the phloem (Dreyer et al., 2017). It too is statistically significantly suppressed in Arabidopsis shoots, but unchanged in *S. parvula* roots and shoots (Figure 6, B and C).

d) *Enhance sequestration into vacuoles*: Vacuolar $[K^+]$ is spatiotemporally regulated primarily by Na^+, K^+/H^+ antiporters, NA^+/H^+ EXCHANGER 1 (NHX1) and NHX2 and secondarily with higher selectivity for K^+ by NHX4 (Bassil et al., 2019). The transcriptional signal to promote K^+ sequestration in Arabidopsis roots or shoots is unclear with mixed regulation among *NHXs* compared to a more coordinated co-expression in *S. parvula* shoots (Figure 6, B and C). Furthermore, Arabidopsis induced *CA^{2+} ACTIVATED OUTWARD RECTIFYING K^+ CHANNEL* (*KCO*) genes encoding K^+-selective vacuolar channel known to release K^+ from vacuoles to the cytosol (Voelker et al., 2006) whereas, *S. parvula*, suppressed *KCO* orthologs implying K^+ sequestration (Figure 6, B and C). Such an attempt is further reinforced by the suppression of tonoplast localized nonselective cation channels CNGC19 and CNGC20 (Yuen and Christopher, 2013) in *S. parvula* roots.

Concordant to decreased photosynthesis, Arabidopsis shoots represent a molecular phenotype suggestive of closed stomata via an induction of *GORK* together with a suppression of guard cell localized POTASSIUM CHANNEL IN ARABIDOPSIS THALIANA 1 (KAT1)/KAT2 (Figure 6, B and C; Ivashikina et al., 2001; Szyroki et al., 2001). Such a molecular phenotype is absent in *S. parvula*. Additionally, a sweeping array of differentially regulated aquaporins and calcium signaling genes were apparent in Arabidopsis compared to limited orthologous responses in *S. parvula* (Supplemental Figure 10). This reinforces our overall depiction of the stress response in *S. parvula* to reflect a more restrained response during excess K^+.

Excess K^+-induced nitrogen starvation in Arabidopsis avoided in *S. parvula*

The reduction in total nitrogen, nitrate, and amino acids in Arabidopsis while those either increased or remained unchanged in *S. parvula* (Figures 2 and 3; Supplemental Figure 6); followed by suppression of amine metabolism-associated genes in Arabidopsis when those were induced in *S. parvula* (Figures 4B and 5C; Supplemental Figure 9B) necessitated further examination on how excess K^+ may alter N-metabolism in plants. Under low $[K^+_{soil}]$, N uptake in the form of nitrate is tightly coupled to K uptake and translocation within the plant. Many of the K and N transporters or their immediate post-transcriptional activators are co-regulated at the transcriptional level (Coskun et al., 2017). We searched for specific transcriptomic cues to determine how N transport was interrupted under high K^+, leading to a deficiency in physiological processes needed to maintain growth or creating a shortage of protective metabolites against oxidative and osmotic stress.

The dual affinity nitrate transporter, NITRATE TRANSPORTER 1.1 (NRT1.1/NPF6.3/CHL1) is the main NO_3^- sensor/transporter accounting for up to 80% of NO_3^- uptake from roots (Feng et al., 2020). Within 3 HAT and onward, *NRT1.1* in Arabidopsis roots is down-regulated (Figure 7A). At low $[NO^-_{3soil}]$, NRT1.1 is activated by CIPK23 to function as a high-affinity NO_3^- transporter (Coskun et al., 2017). In Arabidopsis (and not in *S. parvula*) roots, *CIPK23* is concurrently suppressed with the main K-uptake system formed of *HAK5* and *AKT1-KC1* (Figure 6C). This potentially limits the N content in roots within 24 HAT (Figure 2B). Correspondingly, Arabidopsis roots activated N starvation signals by inducing the expression of genes encoding high-affinity NO_3^- transporters, NRT2.1 and NRT2.4 (O'Brien et al., 2016) despite sufficient N in the growth medium (Figure 7A). Therefore, Arabidopsis showed a molecular phenotype of K^+-induced N-starvation.

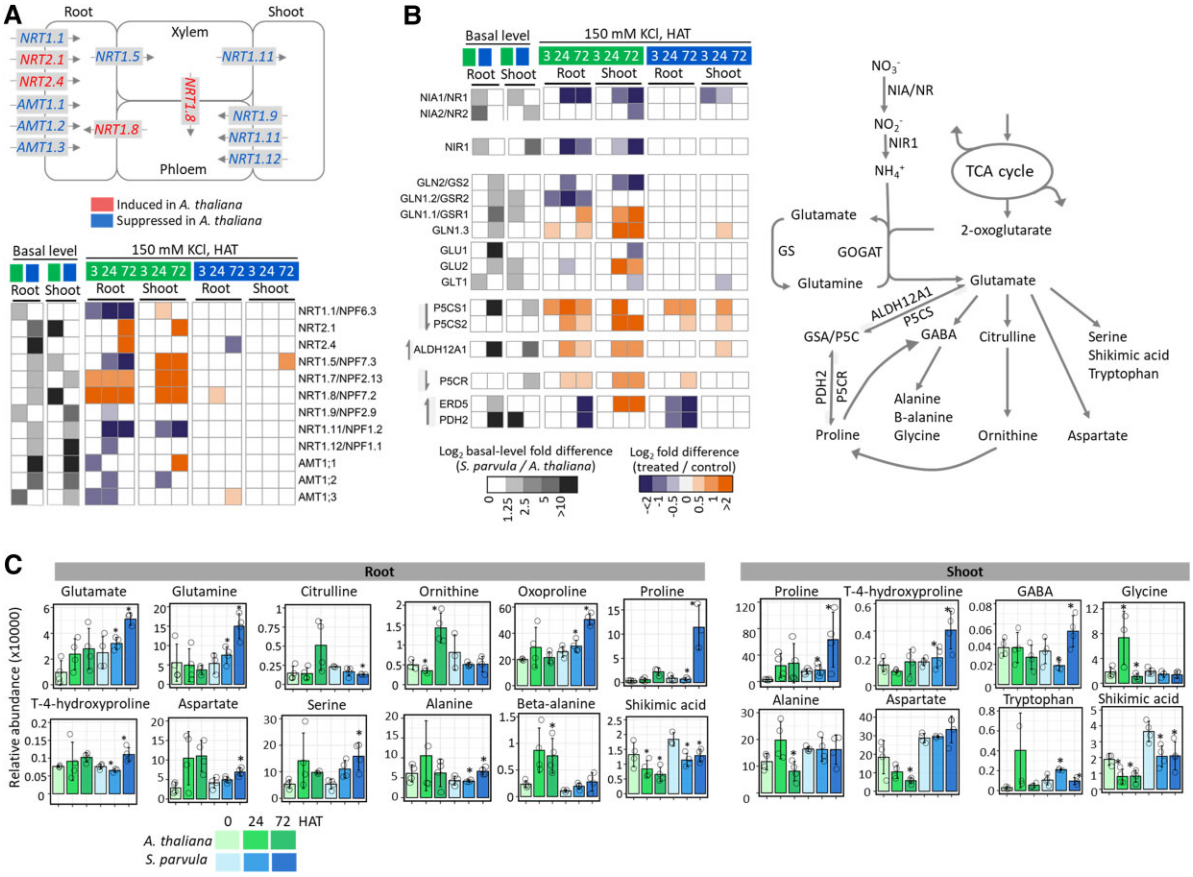

Figure 7 Excess K^+ induced nitrogen starvation and suppressed associated N-assimilation pathways in Arabidopsis compared to *S. parvula*. A, Nitrogen uptake and distribution was severely affected in Arabidopsis upon high K^+. The expression changes associated with major nitrogen transporters in Arabidopsis that regulate root uptake and long-distance transport of N are summarized. B, Coordinated transcriptional regulation showing high K^+-induced suppression of nitrogen assimilation and efforts to accumulate glutamate-derived osmoprotectants. The arrows in front of heatmap blocks indicate the direction of the reaction. C, The primary metabolite pools derived from glutamate in roots and shoots. DEGs at each time point were called using DESeq2 compared to 0 h with a *P*-adj. value based on Benjamini–Hochberg correction for multiple testing set to < 0.01. Significance test for metabolite abundances was performed with one-way ANOVA followed by Tukey's post-hoc test, *P*-value ≤ 0.05. Data are represented as mean of at least three independent replicates $\pm$ SD (≥ 5 hydroponically grown plants per replicate). Open circles indicate the measurement from each replicate. TCA, tricarboxylic acid; HAT, hours after treatment.

The long-distance transport from root to shoot via xylem loading of NO_3^- in roots is primarily regulated via NRT1.5 (NPF7.3) which is a NO_3^-/K^+ cotransporter (Li et al., 2017). In Arabidopsis (and not in *S. parvula*) roots, *NRT1.5* was suppressed possibly in an attempt to limit excess K^+ accumulation in shoots, but consequently depriving NO_3^- in shoots (Figures 2B and 7A). High K^+-induced N-starvation in Arabidopsis was further reflected by its additional transcriptional effort to remobilize NO_3^- internally. For example, *NRT1.7* and *NRT1.8* were induced to promote translocation of NO_3^- from old to young leaves and from xylem back into roots, respectively, while *NRT1.9*, *NRT1.11*, and *NRT1.12* were suppressed to restrict transport via phloem in shoots (Figure 7A; O'Brien et al., 2016). The transcriptional regulatory emphasis on *NRT1.8* is outstanding during excess K^+, given that it is the highest induced gene (104-fold and 73-fold at 24 and 72 HAT, respectively) in the entire Arabidopsis transcriptomic response (Figure 7A; Supplemental Figure 11, Supplemental Table 4). Interestingly, *NRT1.8* is triplicated in *S. parvula* (Oh and Dassanayake, 2019), possibly allowing additional regulatory flexibility to redistribute NO_3^- via the xylem back to the roots. In agreement with our transcriptomic results, the nitrate content was also reduced significantly upon 150 mM KCl treatment for 72 h in Arabidopsis but not in *S. parvula* (Supplemental Figure 6).

NH_4^+ provides another N source and the growth medium included 0.2 mM NH_4^+ compared to 1.4 mM NO_3^-. Therefore, we expected to see transcriptional induction of NH_4^+ transporters to compensate for excess K^+-induced N-starvation in Arabidopsis roots. NH_4^+ and K^+ transport are known to be antagonistically regulated (Coskun et al., 2017). The high-affinity NH_4^+ transporters (AMTs) are inhibited by CIPK23 (Straub et al., 2017). Counterintuitive to our expectations, *AMT1; 1/2/3*, which account for >90% of ammonium uptake into roots (Yuan et al., 2007), were co-suppressed in Arabidopsis (Figure 7A).

We next checked whether the N assimilation pathway from NO_3^- to glutamine via NH_4^+ was also suppressed in *A. thaliana*. Indeed, the genes encoding nitrate reductase (*NIA1/NR1*, *NIA2/NR2*) and nitrite reductase (*NIR*) were coordinately down-regulated in Arabidopsis under high K^+ (Figure 7B). In angiosperms, the main assimilation point of inorganic N to organic compounds is the GS-GOGAT (glutamine synthetase-glutamate synthase) pathway which is tightly coupled to the N and C metabolic state of the plant (O'Brien et al., 2016). The cytosolic *GLN1; 2* and plastidial *GLN2* (coding GS enzymes) together with *GLT* and *GLU1* (coding GOGAT enzymes) were suppressed (Figures 2D and 7B). Contrastingly, the induction of *GLN1; 1* and *GLN1; 3* together with *GLU2* especially in Arabidopsis shoots may reflect an effort to recycle N under N-starved conditions (Figure 7B).

We predicted that the suppression of the N-assimilation pathway would be reflected in the change in primary metabolites derived from glutamate in Arabidopsis. We checked if Arabidopsis had weakened resources to mount appropriate defenses against osmotic and oxidative stress coincident to the depletion of metabolites directly derived from glutamate that are osmolytes and antioxidants (Figure 7C). Both species showed a coordinated effort to accumulate proline and its immediate precursors via induction of key proline biosynthesis genes (Figure 7B, *P5CS1/2*, *P5CR*). However, only *S. parvula* was able to significantly accumulate proline during exposure to excess K^+ (Figure 7C). Proline has dual functions as an osmoprotectant and an antioxidant (Hayat et al., 2012). We see similar pronounced efforts in increasing antioxidant capacity via GABA and beta-alanine (Figure 7, B and C), concordant to increased synthesis of raffinose and myo-inositol against osmotic stress in *S. parvula* (Supplemental Figure 7B). Overall, *S. parvula* is able to accumulate carbon and nitrogen-rich antioxidants and osmoprotectants by maintaining N uptake from roots and N-assimilation pathways independently from the suppressed K-uptake pathways. Contrastingly, the two processes were jointly suppressed in Arabidopsis leading to the depleted N resources (Figure 2B; Supplemental Figure 6) and, in turn, failure to accumulate C and N-rich protective metabolites (Figure 7C).

A previous study showed that orthologous single-copy genes between Arabidopsis and *S. parvula* had generally high sequence similarity even between their syntenic promoter sequences and these were less likely to show differential expression in response to salt stress (Oh et al., 2014). Given the differential expression between some of the main K and nitrate transporter genes identified in the current study, we further checked if their putative promoter sequences lost sequence similarity to noticeable levels. The putative promoter sequences were 2 kb upstream syntenic sequences between gene pairs from translation start site. Several key transporter genes including *NRT1.1* and *NRT1.5* that were down-regulated in Arabidopsis but not differently expressed in *S. parvula* showed clear loss of sequence similarity in their promoters between the two species compared to some key transporters that did not show differential expression in both species (Supplemental Figure 12).

Co-expressed gene clusters indicate stress preparedness in *S. parvula*

We generated co-expressed clusters using 14,318 root and 14,903 shoot ortholog pairs of which, we identified five root and three shoot clusters (Supplemental Figure 13, RC1–5 and SC1-3, respectively; Supplemental Figure 13 and Supplemental Table 12). In three root co-expressed clusters, Arabidopsis orthologs showed a maximum response at 24 HAT, while *S. parvula* showed constitutive responses (Supplemental Figure 13A, RC1-3). These clusters largely represented transcripts associated with stress responses, C and N metabolism, transport, and root development we discussed earlier (Figure 4). The fourth and fifth clusters (Supplemental Figure 13A, RC4-5, 203 ortholog pairs), where *S. parvula* showed a response, comprised functionally uncharacterized genes (37%) that could not be summarized into representative processes. This highlights the extent of functional obscurity of genes that respond to specific ionic stresses minimally characterized in Arabidopsis (Supplemental Figure 13A, RC5), and the previously unexplored regulatory modes detected in orthologs of closely related species whose functional assignment may have been overlooked due to the lack of responses in Arabidopsis (Supplemental Figure 13A, RC4). In all three co-expressed shoot clusters, Arabidopsis again showed a peak response at 24 HAT, while *S. parvula* orthologs showed constitutive expression (Supplemental Figure 13B). The enriched functions in shoot clusters largely overlapped to include stress responses and C and N metabolic processes.

S. parvula showed constitutive expression in all clusters (9,633 orthologs) except in RC4 and RC5, while Arabidopsis showed constitutive expression only in RC4 (76 orthologs; Supplemental Figure 13). Overall, these co-expressed clusters between Arabidopsis and *S. parvula* demonstrate the transcriptome-level stress preparedness in *S. parvula* to facilitate growth and development during excess K^+ stress.

Discussion

Salt tolerance mechanisms against high K^+ are largely unknown compared to the collective understanding for high Na^+ tolerance in plants. Our results demonstrate that high K^+ is more deleterious than Na^+ given at the same external concentrations (Figure 1). Previous studies support this observation noting that excess KCl caused more severe stress symptoms than Na-salts (Eijk, 1939; Ashby and Beadle, 1957; Eshel, 1985; Matoh et al., 1986; Cramer et al., 1990; Wang et al., 2001; Ramos et al., 2004; Richter et al., 2019; Zhao et al., 2020). The canonical adaptations described for salt tolerance mechanisms associated with NaCl-induced salt stress (Pantha and Dassanayake, 2020) are insufficient to explain adaptations required for KCl-induced salt stress.

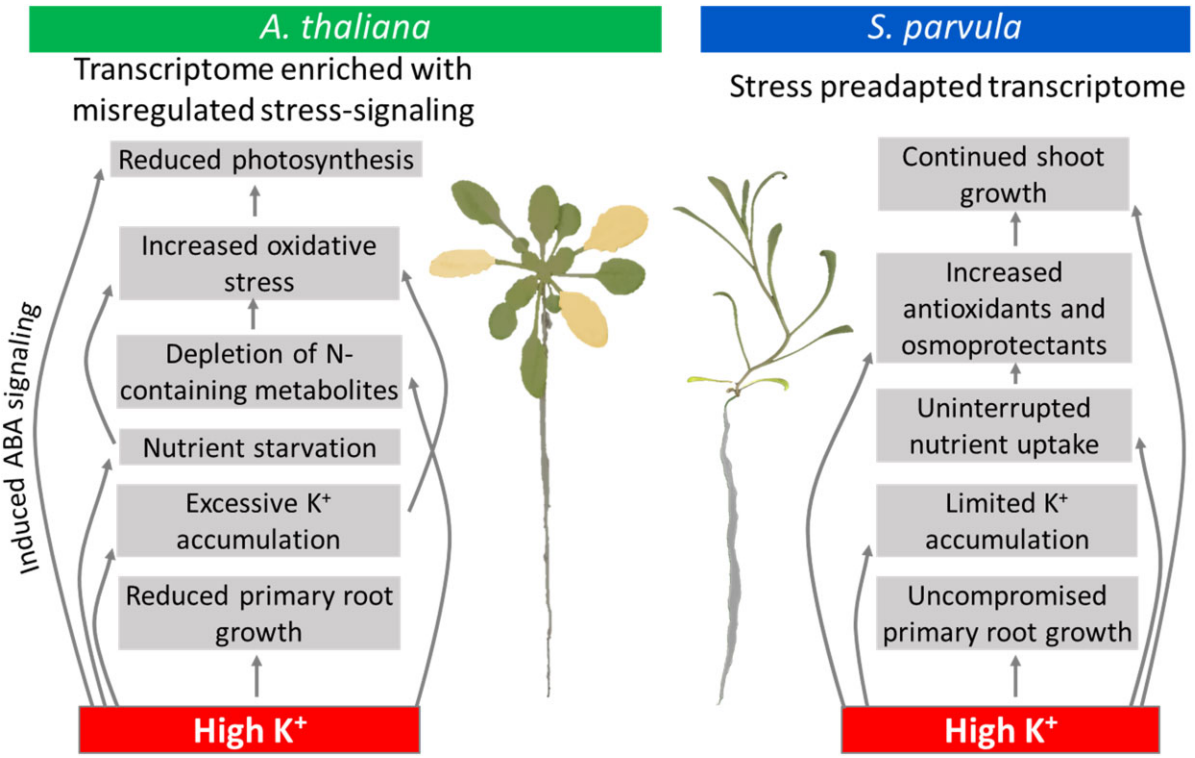

Figure 8 Processes deduced from the multiomics study, physiological assessments, and inferences made for confirmed gene functions in Arabidopsis that collectively suggest major differences between stress-resilient and stress-sensitive growth under high potassium-induced salinity stress.

The extremophyte, *S. parvula,* amidst high K^+ can sustain its growth and development; compartmentalize excess K in roots instead of in shoots; maintain uninterrupted nutrient uptake; increase its antioxidants and osmoprotectants; decouple transcriptional regulation between K and N transport; and coordinately induce abiotic stress response pathways along with growth promoting pathways (Figure 8). Contrastingly, the more stress-sensitive plant, Arabidopsis shows, interrupted growth; excessive accumulation of K^+ in roots and shoots; depletion of essential nutrients; depletion of N-containing metabolites; and sweeping transcriptomic adjustments suggesting initiation of autophagy, ROS accumulation, induction of both abiotic and biotic stresses, and responses to all major hormone pathways (Figure 8). Based on our comparative analyses, we propose two deterministic steps in the overall stress response sequence to survive high K^+ stress.

Surviving K toxicity by avoiding N starvation

K is a macronutrient and plants have evolved many functionally redundant transporters to uptake K^+ into roots and redistribute within plants (Shabala and Cuin, 2008). When external [K^+] exceed physiologically optimal conditions, it is not surprising that the immediate response from both plants was to suppress expression of K^+ transporters that primarily control K^+ influx into roots (Figure 6). Additionally, *S. parvula* down-regulated nonselective CNGCs that may be permeable to K^+ in roots. Several CNGCs are reported to allow Na^+ or K^+ transport and have been implicated in their functions during Na-induced salt stress by controlling Na influx into roots. However, their functional and spatiotemporal specificity remains largely unresolved (Dietrich et al., 2020) and needs to be determined before evaluating how selected CNGCs may be involved in limiting excess K influx under K-induced salt stress.

Arabidopsis further seems to suppress long-distance transport of K^+ via NRT1.5 that co-transports NO_3^- and K^+ (Li et al., 2017). NO_3^- is transported as a counterion with K^+ in root to shoot translocation as described by the "Dijkshoorn–Ben Zioni model" (Dijkshoorn et al., 1968; Zioni et al., 1971; Coskun et al., 2017). The suppression of *NRT1.5* limits NO_3^- remobilization in plants (Chen et al., 2012). This interference to N transport within the plant is compounded by the transcriptional co-suppression of NRT and AMT transporters known to limit N intake from soil (Figure 7; Tegeder and Masclaux-Daubresse, 2018). This creates an N-starved condition for Arabidopsis not observed for *S. parvula* (Figure 2 ;Supplemental Figure 6). During limiting K^+ conditions, N-uptake is down-regulated to prevent excess N-induced toxicity in plants as a favorable mechanism to adapt to K^+-starvation (Armengaud et al., 2004). This interdependent N and K transport and regulation favorable at low [K^+_{soil}] appear to be detrimental at high [K^+] as it creates an antagonistic pleiotropic effect (condition-dependent traits that can cause positive as well as negative impacts).

We observed a significant induction of *NRT1.8/NPF7.2* suggestive of an effort to reimport N from the stele in

Arabidopsis (Li et al., 2010). However, this transcriptional effort did not cascade to the ionomic level (Figure 2, B and D; Supplemental Figure 6). N remobilization via induction of *NRT1.8* while concurrently suppressing *NRT1.5* (Figure 7A) during N starvation is regulated by ethylene-jasmonic acid signaling together with low N-sensing by nitrate reductase (Chen et al., 2012; Zhang et al., 2014). Both ethylene and jasmonic acid signaling are among the enriched differently regulated transcriptional processes in Arabidopsis (Figure 4B). Interestingly, *S. parvula* appears to have a more flexible and effective regulatory capacity to allow N-uptake decoupled from restricted K-uptake and it does not suppress internal remobilization of NO_3^- and K^+ via NRT1.5 (Figures 6 and 7). This may prevent *S. parvula* from experiencing a high-, K-induced N-starvation.

The depletion of N uptake in Arabidopsis further cascades into depletion of primary metabolites containing N (Figure 3D) with a concomitant transcriptional suppression observed in N assimilation via the GS-GOGAT pathway (Figure 7; O'Brien et al., 2016; Ji et al., 2019). This not only creates a shortage of essential primary metabolites required for growth and development but also depletes essential antioxidants and osmolytes to defend against the mounting oxidative and osmotic stresses (Figures 3, 4, B–D, 7, and 8)., High K in the growth medium is known to exert osmotic and oxidative stress (Osakabe et al., 2013; Zheng et al., 2013). This creates an overall need to boost osmotic and antioxidant defense systems to successfully survive high K^+ toxicity.

Synergistic transcriptional and metabolic resource allocation to increase osmoprotectants during high K^+ is much more pronounced in *S. parvula* than in Arabidopsis (Figures 3 and 7). Proline accumulation resulting from increased synthesis and reduced catabolism have been widely shown as a key adaptation during salt stress (Kishor et al., 1995; Gong et al., 2005; Kant et al., 2006; Kumar et al., 2010; Hayat et al., 2012).

K and N regulate phosphorus uptake (Coskun et al., 2017; Maeda et al., 2018; Cui et al., 2019), while K^+ toxicity can induce P-starvation (Ródenas et al., 2019). Arabidopsis experienced severe shortages of multiple key nutrient depletions (Figure 2 and Supplemental Figure 6), which *S. parvula* seemingly avoided by having independent regulatory capacity of K and N uptake (Figures 6–8). Therefore, we propose that the ability to regulate independent K^+ uptake is a key deterministic step toward building resilience to excess K^+.

Avoiding transcriptional misregulation of K^+ signaling

Multiple hormonal pathways use K^+ for developmental, biotic stress, and abiotic stress signaling (Zhang et al., 2014; Hauser et al., 2017; Shabala, 2017). Canonical mechanisms involving K^+ signaling for growth are based on sensing external K^+ at low or favorable conditions. When supplied with toxic levels of K^+, Arabidopsis induced nonselective hormone signaling pathways inept to the extant stress (Figure 4) indicative of transcriptional misregulation. Therefore, we propose that the capacity to avoid transcriptional misregulation of K^+ signaling is the second major deterministic step in surviving high K^+ stress. If unavoided, it can lead to systemic damage via activation of ROS and autophagy pathways, as demonstrated by Arabidopsis with its increased ROS accumulation perhaps resulting from induction of futile biotic stress responses or unmitigated oxidative stresses induced by high K^+ detrimental especially at a nutrient starved environment (Figure 4). ROS accumulation combined with autophagy are associated with abiotic and biotic stress responses and developmental processes (Liu et al., 2005; Thompson et al., 2005; Lv et al., 2014; Pantha and Dassanayake, 2020). However, uncontrolled initiation of autophagy signifies a failed stress response strategy (Floyd et al., 2015). In Arabidopsis shoots, autophagy is the most enriched transcriptional pathway. The collective transcriptional signal enriched for lipid catabolism, protein degradation, DNA repair, cell death, and leaf senescence (Das and Roychoudhury, 2014; Figure 4B) likely preceding phenotypic changes expected under long-term exposure to high to excess K^+ further indicates the maladaptive stress response shown by Arabidopsis contrasted against a preadapted state observed for *S. parvula* (Figures 5 and 8). Previous transcriptome and metabolome characterizations from extremophytes including *S. parvula* have shown similar stress-ready states for other abiotic stresses (Kant et al., 2006; Lugan et al., 2010; Oh et al., 2014; Wang et al., 2021). Future studies targeting long-term exposure to excess K^+ complementing the current study will be needed to critically evaluate adaptive traits that are deterministic for plant survival in high K^+ environments.

In conclusion, upon exposure to high K^+, plants undergo physiological, metabolic, and transcriptional changes and a subset of those changes lead to stress adaptive traits while the other responses are indicative of failed molecular phenotypes unable to meet the increasing systemic toxicity exerted by excess K^+ accumulation. The deterministic steps whether a plant would be able to survive K-induced salt stress or descend into unmitigated stress responses were primarily dictated by the ability to regulate K uptake independent from other nutrient uptake pathways while avoiding deleterious signaling processes. This decoupled regulation of K transport and stress signaling can be targeted to design improved crops that are better able to dynamically adjust to a wide array of soils or irrigation water sources with different salt compositions increasingly comprised high K^+ in freshwater-limited environments.

Materials and methods

Detailed methods are given in Supplemental Methods.

Plant material

Arabidopsis (*Arabidopsis thaliana*; Col-0) and *S. parvula* (Lake Tuz) were grown in controlled environments hydroponically, on plates, or in soil at 23°C, 12/12 h light/dark, and 60% relative humidity (Wang et al., 2021). Multiomics

data were generated from plants grown in 1/5th Hoagland's solution which included 1.2 mM K^+ to support plant growth in all conditions. Supplemental KCl (150 mM) treatments provided excess K^+ beyond its expected range serving as a nutrient (0.1–6 mM; Ashley et al., 2006). Tissues were harvested at 0, 3, 24, and 72 HAT for ionomic, metabolomic, and transcriptomic profiling (Supplemental Figure 1). All samples were harvested at the same time and were 28-day-old when used for –omics data generation with 3–5 biological replicates for each treatment.

Physiological assessments

Root growth assessments were made using plate-grown seedlings scanned and processed with ImageJ (Ferreira and Rasband, 2012). Propidium iodide stained roots were imaged using a Leica SP8 confocal microscope following Fulcher and Sablowski (2009). Reproductive stage assessments were taken from soil grown plants treated with 0–400 mM NaCl or KCl given for at least 2 weeks. CO_2 assimilation rates were measured on hydroponically grown plants using an infrared gas analyzer (LI-6400XT, LI-COR, Lincoln, USA). Leaves were stained for H_2O_2 and O_2^- using 3,3′-diaminobenzidine and nitroblue tetrazolium as described in Jabs et al. (1996) and Daudi and O'Brien (2012). Nitrate quantification was conducted on plate-grown 5-day-old seedlings treated with 0, 100, 150 mM KCl for 72 h as detailed in Supplemental Methods.

Elemental profiling

Samples were processed following Ziegler et al. (2013) to quantify K, P, Mg, S, Ca, Al, Zn, Co, Ni, Fe, Se, Cu, B, Mn, Mo, As, Rb, Cd, Na, Li, and Sr via inductively coupled plasma mass spectrometry (Baxter et al., 2014). Carbon and nitrogen were quantified using a Costech 4,010 elemental analyzer (Costech, Valencia, USA). Significant differences were calculated based on one-way ANOVA, followed by Tukey's post-hoc test ($P \leq 0.05$) using agricolae and visualized as heatmaps using pheatmap (R packages, v. 1.0.12; Kolde, 2012).

Metabolite profiling

Nontargeted high throughput metabolite profiling was conducted on frozen samples using gas chromatography-mass spectrometry (Fiehn et al., 2008). Additional details on metabolite annotation and quantification are given in Supplemental Methods. Significance tests were performed as described for ionomics and visualized using circlize, R (Gu et al., 2014). MACs between control (0 HAT) and KCl treated conditions were calculated with one-way ANOVA followed by Tukey's post-hoc test, P-value ≤ 0.05.

RNA-seq analyses

Total RNA was extracted from triplicates of root and shoot tissues harvested at 0, 3, 24, and 72 HAT with 150 mM KCl (Supplemental Figure 1). Strand-specific RNA-seq libraries were sequenced on Illumina HiSeq4000. Reads uniquely mapped to Arabidopsis TAIR10 or *S. parvula* (Dassanayake et al., 2011) v2.2 gene models (https://phytozome-next.jgi.doe.gov/; Supplemental Table 3) were counted for identifying DEGs based on DESeq2 (Love et al., 2014) at P-adj. < 0.01 comparing each time point with the control sample (0 HAT). Orthologous gene pairs were identified using CLfinder-OrthNet (Oh and Dassanayake, 2019) and further refined as described in Wang et al. (2021). Median normalized expression of orthologs was used to determine temporal co-expression clusters based on fuzzy k-means clustering (Gasch and Eisen, 2002). Enriched functional groups were identified using BinGO (Maere et al., 2005; P-adj. ≤ 0.05) and further summarized to nonredundant functional groups using GOMCL (Wang et al., 2020).

Accession numbers

Sequences of all genes associated with this article can be found with relevant accession numbers available in The Arabidopsis Information Resource database and listed in Supplemental Table 4. Additionally, genes highlighted in this article can be found under accession numbers: *AKT1*, AT2G26650; *AKT2/3*, AT4G22200; *AMT1; 1*, AT4G13510; *AMT1; 2*, AT1G64780; *AMT1; 3*, AT3G24300; *ARF2*, AT5G62000; *ATKCO1; 1*, AT5G55630; *CBL1*, At4g17615; *CBL9*, At5g47100; *CIPK23*, At1g30270; *CNGC10*, AT1G01340; *CNGC12*, AT2G46450; *CNGC13*, AT4G01010; *CNGC19*, AT3G17690; *CNGC20*, AT3G17700; *CNGC3*, AT2G46430; *GLN1.1/GSR1*, AT5G37600; *GLN1.2/GSR2*, AT1G66200; *GLN1.3*, AT1G17290; *GLT1*, At5g53460; *GLU1*, At5g04140; *GLU2*, At2g41220; *GORK*, AT5G37500; *GS2/GLN2*, AT5G35630; *HAK5*, AT4G13420; *KAT1*, AT5G46240; *KC1/KAT3*, AT4G32650; *KCO2*, AT5G46370; *KUP6*, AT1G70300; *KUP7*, AT5G09400; *KUP8*, AT5G14880; *NHX1*, AT5G27150; *NHX2*, AT3G05030; *NIA1/NR1*, AT1G77760; *NIA2/NR2*, AT1G37130; *NPF1.1/NRT1.12*, AT3G16180; *NPF1.2/NRT1.11*, AT1G52190; *NPF1.2/NRT1.11*, AT1G52190; *NPF2.13/NRT1.7*, At1G69870; *NPF2.9/NRT1.9*, AT1G18880; *NPF6.3/NRT1.1*, AT1G12110; *NPF7.2/NRT1.8*, AT4G21680; *NPF7.2/NRT1.8*, AT4G21680; *NPF7.3/NRT1.5*, AT1G32450; *NRT2.1*, AT1G08090; *NRT2.4*, AT5G60770; *P5CR*, AT5G14800; *P5CS1*, AT2G39800; *P5CS2*, AT3G55610; *RAP2.11*, AT5G19790; *SKOR*, AT3G02850; *SOS1*, AT2G01980.

Data availability

The RNA-seq reads generated in this study are available at NCBI-SRA database under BioProject PRJNA63667. Mapped transcripts from this study for *S. parvula* can be browsed at https://www.lsugenomics.org/genome-browser.

Supplemental data

The following materials are available in the online version of this article.

Supplemental Methods. Additional methods information.

Supplemental Figure S1. Sampling scheme for the ionome, metabolome, and transcriptome experiments performed in this study.

Supplemental Figure S2. KCl is more toxic than NaCl at the same osmotic strength shown by salt treatments extended to two weeks.

Supplemental Figure S3. Root traits showing KCl is more toxic than NaCl at the same osmotic strength.

Supplemental Figure S4. KCl, KNO_3, and K_2SO_4 showed similar growth responses at comparable osmotic strengths.

Supplemental Figure S5. Cell viability during 150 mM KCl treatments.

Supplemental Figure S6. Total potassium and nitrate content in Arabidopsis and *S. parvula*.

Supplemental Figure S7. Carbohydrate and nitrogen metabolism related processes were enriched in *S. parvula* roots.

Supplemental Figure S8. Overview of transcriptomes in each condition tested in response to high K stress in Arabidopsis and *S. parvula* roots.

Supplemental Figure S9. The majority of differentially expressed genes (DEGs) show species specific responses followed by tissue and response time specificity.

Supplemental Figure S10. Genes coding for calcium signaling and aquaporins are differently regulated during high K^+ stress.

Supplemental Figure S11. Normalized expression of *GORK*, *SOS1*, *HKT1*, and *NRT1.8* in indicated tissues of Arabidopsis and *S. parvula* under 150 mM KCl treatments.

Supplemental Figure S12. Comparison of putative promoter sequences for selected K and Nitrogen transporter genes discussed in the current study.

Supplemental Figure S13. Co-expressed ortholog gene modules highlight stress preparedness toward high K^+ stress in *S. parvula* orthologs that are constitutively expressed compared to induction or suppression of orthologs in Arabidopsis.

Supplemental Table S1. Elemental quantification of Arabidopis and *Schrenkiella parvula* root and shoot.

Supplemental Table S2. Relative abundance of metabolites for Arabidopsis and *S. parvula* roots and shoots sample.

Supplemental Table S3. Number of total reads and percentage of uniquely mapped reads to Arabidopsis (TAIR10) or *S. parvula* v2.2 gene models for root and shoot transcriptomes under high K^+.

Supplemental Table S4. List of differentially expressed genes (DEGs) in 3, 24, and 72 hours after treatment (HAT) in Arabidopsis and *S. parvula* root and shoot.

Supplemental Table S5. Enriched biological processes for a nonredundant set of induced and suppressed DEGs for Arabidopsis roots and shoots sample under 150 mM KCl.

Supplemental Table S6. Enriched biological processes for time point-specific DEGs (3, 3&24 + 24, 24&72, 72, and 3&24&72) for Arabidopsis roots sample under 150 mM KCl.

Supplemental Table S7. Enriched biological processes for time point-specific DEGs (3, 3&24 + 24, 24&72, 72, and 3&24&72) for Arabidopsis shoots sample under 150 mM KCl.

Supplemental Table S8. Enriched biological processes for time point-specific (3, 3&24, 24, 24&72, 72, and 3&24&72) induced and suppressed DEGs for Arabidopsis roots sample under 150 mM KCl.

Supplemental Table S9. Enriched biological processes for time point-specific (3, 3&24, 24, 24&72, 72, and 3&24&72) induced and suppressed DEGs for Arabidopsis shoots sample under 150 mM KCl.

Supplemental Table S10. Enriched biological processes for diametric responses (i.e. genes that are induced in one species when their orthologs are suppressed in the other species) in Arabidopsis and *S. parvula* roots and shoots sample under 150 mM KCl.

Supplemental Table S11. Enriched biological processes for a nonredundant set of induced and suppressed DEGs for *S. parvula* roots and shoots sample under 150 mM KCl.

Supplemental Table S12. Normalized gene expression clusters of ortholog pairs (OP) between Arabidopsis and *S. parvula* in roots and shoots sample.

Author contributions

P.P. conducted experiments and performed data analyses. D.L. supervised and assisted with measuring CO_2 assimilation rates. D.H.O. provided bioinformatics assistance. M.D. developed the experimental design and supervised the overall project. P.P. and M.D. interpreted results and wrote the article with input from all co-authors who revised and approved the final manuscript.

Acknowledgments

We thank Drs. Guannan Wang, Kieu-Nga Tran, Aaron Smith, and John Larkin, and Chathura Wijesinghege for providing feedback on the manuscript and facilitating helpful discussions; Prava Adhikari for additional assistance with phenotyping, and undergraduate students Saad Chaudhari, Megan Guilbeau, and August Steinkamp for their assistance to grow plants. We acknowledge LSU High Performance Computing services for providing computational resources, and Drs. John Cheeseman and Alvaro Hernandez for their assistance with sequencing services at the University of Illinois.

Funding

This work was supported by the US National Science Foundation awards MCB-1616827 and IOS-EDGE-1923589, US Department of Energy BER-DE-SC0020358, and the Next-Generation BioGreen21 Program of Republic of Korea (PJ01317301) awarded to M.D. P.P. was supported by an Economic Development Assistantship award from Louisiana State University.

Conflict of interest statement. None declared.

References

IPCC (2021) Climate change 2021: the physical science basis. Contribution of Working Group I to the Sixth Assessment Report of the Intergovernmental Panel on Climate Change, 207. Cambridge University Press, Switzerland

Arienzo M, Christen EW, Quayle W, Kumar A (2009) A review of the fate of potassium in the soil-plant system after land application of wastewaters. J Hazard Mater **164**(2–3): 415–422

Armengaud P, Breitling R, Amtmann A (2004) The potassium-dependent transcriptome of Arabidopsis reveals a prominent role of jasmonic acid in nutrient signaling. Plant Physiol **136**(1): 2556–2576

Ashby WC, Beadle NCW (1957) Studies in halophytes : III. Salinity factors in the growth of Australian saltbushes. Ecology **38**(2): 344–352

Ashley MK, Grant M, Grabov A (2006) Plant responses to potassium deficiencies: a role for potassium transport proteins. J Exp Bot **57**(2): 425–436

Bassil E, Zhang S, Gong H, Tajima H, Blumwald E (2019) Cation specificity of vacuolar NHX-type cation/H + antiporters 1. Plant Physiol **179**(2): 616–629

Baxter IR, Ziegler G, Lahner B, Mickelbart M V, Foley R, Danku J, Armstrong P, Salt DE, Hoekenga OA (2014) Single-kernel ionomic profiles are highly heritable indicators of genetic and environmental influences on elemental accumulation in maize grain (Zea mays). PLoS One **9**(1): e87628

Chen CZ, Lv XF, Li JY, Yi HY, Gong JM (2012) Arabidopsis NRT1.5 is another essential component in the regulation of nitrate reallocation and stress tolerance. Plant Physiol **159**(4): 1582–1590

Coskun D, Britto DT, Kronzucker HJ (2017) The nitrogen–potassium intersection: membranes, metabolism, and mechanism. Plant Cell Environ **40**(10): 2029–2041

Cramer GR, Epstein E, Lauchli A (1990) Effects of sodium, potassium and calcium on salt-stressed barley. I. Growth analysis. Physiol Plant **80**(1): 83–88

Cui Y, Li X, Yuan J, Wang F, Wang S (2019) Biochemical and biophysical research communications nitrate transporter NPF7.3/NRT1.5 plays an essential role in regulating phosphate deficiency responses in Arabidopsis. Biochem Biophys Res Commun **508**(1): 314–319

Das K, Roychoudhury A (2014) Reactive oxygen species (ROS) and response of antioxidants as ROS-scavengers during environmental stress in plants. Front Environ Sci **2**(December): 1–13

Dassanayake M, Oh D-H, Haas JS, Hernandez A, Hong H, Ali S, Yun D-J, Bressan RA, Zhu J-K, Bohnert HJ, et al. (2011) The genome of the extremophile crucifer *Thellungiella parvula*. Nat Genet **43**(9): 913–918

Daudi A, O'Brien JA (2012) Detection of hydrogen peroxide by DAB staining in Arabidopsis leaves. Bio Protoc **2**(18): e263

David ACM (2010) Mineral sources of potassium for plant nutrition. A review. Agron Sustain Dev Dev **30**(2): 281–294

Demidchik V, Straltsova D, Medvedev SS, Pozhvanov GA, Sokolik A, Yurin V (2014) Stress-induced electrolyte leakage: the role of K +-permeable channels and involvement in programmed cell death and metabolic adjustment. J Exp Bot **65**(5): 1259–1270

Dietrich P, Moeder W, Yoshioka K (2020) Plant cyclic nucleotide-gated channels: new insights on their functions and regulation. Plant Physiol **184**(1): 27–38

Dijkshoorn W, Lathwell DJ, Wit CTDE (1968) Temporal changes in carboxylate content of ryegrass with stepwise change in nutrition. Plant Soil **29**(3): 369–390

Dreyer I, Gomez-Porras JL, Riedelsberger J (2017) The potassium battery: a mobile energy source for transport processes in plant vascular tissues. New Phytol **216**(4): 1049–1053

Duval JS, Carson JM, Holman PB, Darnley AG (2005) Terrestrial radioactivity and gamma-ray exposure in the United States and Canada. U.S. Geological Survey Open-File Report 2005-1413. Available online only.

Eijk VM (1939) Analysis of the effect of NaCl on development, succulence and transpiration in Salicornia herbacea, as well as studies on the influence of salt uptake on root respiration in Aster Tripolium. Recl des Trav Bot néerlandais **36**(2): 559–657

Eshel A (1985) Response of Suaeda aegyptiaca to KCl, NaCl and Na2SO4 treatments. Physiol Plant **64**(3): 308–315

Feng H, Fan X, Miller AJ, Xu G (2020) Plant nitrogen uptake and assimilation: regulation of cellular pH homeostasis. J Exp Bot **71**(15): 4380–4392

Ferreira T, Rasband W (2012) ImageJ User Guide-IJ 1.46. https://imagej.nih.gov/ij/docs/guide/user-guide.pdf

Fiehn O, Wohlgemuth G, Scholz M, Kind T, Lee DY, Lu Y, Moon S, Nikolau B (2008) Quality control for plant metabolomics: reporting MSI-compliant studies. Plant J **53**(4): 691–704

Floyd BE, Pu Y, Soto-Burgos J, Bassham DC (2015) Plant Programmed Cell Death

Fulcher N, Sablowski R (2009) Hypersensitivity to DNA damage in plant stem cell niches. Proc Natl Acad Sci U S A **106**(49): 20984–20988

Gasch AP, Eisen MB (2002) Exploring the conditional coregulation of yeast gene expression through fuzzy k-means clustering. Genome Biol. **3**(11): research0059.1

Gaymard F, Pilot G, Lacombe B, Bouchez D, Bruneau D, Boucherez J, Michaux-Ferrière N, Thibaud JB, Sentenac H (1998) Identification and disruption of a plant shaker-like outward channel involved in K+ release into the xylem sap. Cell **94**(5): 647–655

Gierth M, Mäser P, Schroeder JI (2005) The potassium transporter AtHAK5 functions in K+ deprivation-induced high-affinity K+ uptake and AKT1 K+ channel contribution to K+ uptake kinetics in Arabidopsis roots. Plant Physiol **137**(3): 1105–1114

FAO (2021) Global map of salt-affected soils: GSASmap V1.0. FAO 20

Gobert A, Park G, Amtmann A, Sanders D, Maathuis FJM (2006) Arabidopsis thaliana cyclic nucleotide gated channel 3 forms a non-selective ion transporter involved in germination and cation transport. J Exp Bot **57**(4): 791–800

Gong Q, Li P, Ma S, Indu Rupassara S, Bohnert HJ (2005) Salinity stress adaptation competence in the extremophile *Thellungiella halophila* in comparison with its relative Arabidopsis thaliana. Plant J **44**(5): 826–839

Gu Z, Gu L, Eils R, Schlesner M, Brors B (2014) Circlize implements and enhances circular visualization in R. Bioinformatics **30**(19): 2811–2812

Guo K, Babourina O, Christopher DA, Borsics T, Rengel Z (2008) The cyclic nucleotide-gated channel, AtCNGC10, influences salt tolerance in Arabidopsis. Physiol Plant **134**(3): 499–507

FAO (2022) Halt soil salinization, boost soil productivity—Proceedings of the Global Symposium on Salt-affected Soils

Han M, Wu W, Wu WH, Wang Y (2016) Potassium transporter KUP7 is involved in K+ acquisition and translocation in Arabidopsis root under K+-limited conditions. Mol Plant **9**(3): 437–446

Hauser F, Li Z, Waadt R, Schroeder JI (2017) Snapshot: abscisic acid signaling. Cell **171**(7): 1708–1708.e0

Hayat S, Hayat Q, Alyemeni MN, Wani AS, Pichtel J, Ahmad A (2012) Role of proline under changing environments. Plant Signal Behav **7**-(11): 1456–1466

Ivashikina N, Dirk B, Ache P, Meyerho O, Felle HH, Hedrich R (2001) K+ channel profile and electrical properties of Arabidopsis root hairs. FEBS Lett **508**(3): 463–469

Jabs T, Dietrich RA, Dangl JL (1996) Initiation of runaway cell death in an Arabidopsis mutant by extracellular superoxide. Science **273**-(5283): 1853–1856

Ji Y, Li Q, Liu G, Selvaraj G, Zheng Z, Zou J, Wei Y (2019) Roles of cytosolic glutamine synthetases in arabidopsis development and stress responses. Plant Cell Physiol **60**(3): 657–671

Jobbágy EG, Jackson RB (2001) The distribution of soil nutrients with depth : global patterns and the imprint of plants. Biogeochemistry **53**(1): 51–77

Kant S, Kant P, Raveh E, Barak S (2006) Evidence that differential gene expression between the halophyte, *Thellungiella halophila*, and Arabidopsis thaliana is responsible for higher levels of the compatible osmolyte proline and tight control of Na+ uptake in T. halophila. Plant, Cell Environ **29**(7): 1220–1234

Kim MJ, Ruzicka D, Shin R, Schachtman DP (2012) The Arabidopsis AP2/ERF transcription factor RAP2.11 modulates plant response to low-potassium conditions. Mol Plant **5**(5): 1042–1057

Kishor PBK, Hong Z, Miao C-H, Hu C-AA, Verma DPS (1995) Overexpression of A1-pyrroline-5-carboxylate synthetase increases proline production and confers osmotolerance in transgenic plants. Plant Physiol **108**(4): 1387–1394

Kolde R (2012) pheatmap v.1.0.8. https://cran.r-project.org/package=pheatmap 1–7

Kresge PO, Gavlak RG, Custer SG, Robbins CW, Jacobsen JS (1988) Identification and impact of excess soil potassium oncrop and livestock nutrition. Proceedings, 39th Annual Far West Regional Fertilizer Conference

Kumar V, Shriram V, Kishor PBK, Jawali N, Shitole MG (2010) Enhanced proline accumulation and salt stress tolerance of transgenic indica rice by over-expressing P5CSF129A gene. Plant Biotechnol Rep **4**(1): 37–48

Lequeux H, Hermans C, Lutts S, Verbruggen N (2010) Response to copper excess in Arabidopsis thaliana: impact on the root system architecture, hormone distribution, lignin accumulation and mineral profile. Plant Physiol Biochem **48**(8): 673–682

Li JY, Fu YL, Pike SM, Bao J, Tian W, Zhang Y, Chen CZ, Zhang Y, Li HM, Huang J, et al. (2010) The Arabidopsis nitrate transporter NRT1.8 functions in nitrate removal from the xylem sap and mediates cadmium tolerance. Plant Cell **22**(5): 1633–1646

Li H, Yu M, Du XQ, Wang ZF, Wu WH, Quintero FJ, Jin XH, Li HD, Wang Y (2017) NRT1.5/NPF7.3 functions as a proton-coupled H +/K+ antiporter for K+ loading into the xylem in arabidopsis. Plant Cell **29**(8): 2016–2026

Liu Y, Schiff M, Czymmek K, Tallóczy Z, Levine B, Dinesh-Kumar SP (2005) Autophagy regulates programmed cell death during the plant innate immune response. Cell **121**(4): 567–577

Love MI, Huber W, Anders S (2014) Moderated estimation of fold change and dispersion for RNA-seq data with DESeq2. Genome Biol **15**(12): 550

Lugan R, Niogret MF, Leport L, Guégan JP, Larher FR, Savouré A, Kopka J, Bouchereau A (2010) Metabolome and water homeostasis analysis of *Thellungiella salsuginea* suggests that dehydration tolerance is a key response to osmotic stress in this halophyte. Plant J **64**(2): 215–229

Lv X, Pu X, Qin G, Zhu T, Lin H (2014) The roles of autophagy in development and stress responses in Arabidopsis thaliana. Apoptosis **19**(6): 905–921

Maeda Y, Konishi M, Kiba T, Sakuraba Y, Sawaki N, Kurai T, Ueda Y, Sakakibara H, Yanagisawa S (2018) A NIGT1-centred transcriptional cascade regulates nitrate signalling and incorporates phosphorus starvation signals in Arabidopsis. Nat Commun **9**(1): 1–14

Maere S, Heymans K, Kuiper M (2005) BiNGO: a cytoscape plugin to assess overrepresentation of gene ontology categories in biological networks. Bioinformatics **21**(16): 3448–3449

Matoh T, Watanabe J, Takahashi E (1986) Effects of sodium and potassium salts on the growth of a halophyte. Soil Sci Plant Nutr **32**(3): 451–459

Nilhan TG, Emre YA, Osman K (2008) Soil determinants for distribution of Halocnemum strobilaceum Bieb. (Chenopodiaceae) around Lake Tuz, Turkey. Pakistan J Biol Sci **11**(4): 565–570

Nishizawa A, Yabuta Y, Shigeoka S (2008) Galactinol and raffinose constitute a novel function to protect plants from oxidative damage. Plant Physiol **147**(3): 1251–1263

O'Brien JAA, Vega A, Bouguyon E, Krouk G, Gojon A, Coruzzi G, Gutiérrez RAA (2016) Nitrate transport, sensing, and responses in plants. Mol Plant **9**(6): 837–856

Oh D-H, Dassanayake M (2019) Landscape of gene transposition–duplication within the Brassicaceae family. DNA Res **26**(1): 21–36

Oh D-H, Hong H, Lee SY, Yun D-J, Bohnert HJ, Dassanayake M (2014) Genome structures and transcriptomes signify niche adaptation for the multi-ion tolerant extremophyte *Schrenkiella parvula*. Plant Physiol **164**(4): 2123–2138

Oh D-H, Leidi E, Zhang Q, Hwang S-M, Li Y, Quintero FJ, Jiang X, D'Urzo MP, Lee SY, Zhao Y, et al. (2009) Loss of halophytism by interference with SOS1 expression. Plant Physiol **151**(1): 210–222

Osakabe Y, Arinaga N, Umezawa T, Katsura S, Nagamachi K, Tanaka H, Ohiraki H, Yamada K, Seo S-U, Abo M, et al. (2013) Osmotic stress responses and plant growth controlled by potassium transporters in Arabidopsis. Plant Cell **25**(2): 609–624

Pantha P, Dassanayake M (2020) Living with salt. Innov **1**(3): 100050

Ragel P, Ródenas R, García-martín E, Andrés Z, Villalta I, Nieves-cordones M, Rivero RM, Martínez V, Pardo JM, Quintero FJ, et al. (2015) The CBL-interacting protein kinase CIPK23 regulates HAK5-mediated high-affinity K+ uptake in Arabidopsis roots. Plant Physiol **169**(4): 2863–2873

Ramos J, López MJ, Benlloch M (2004) Effect of NaCl and KCl salts on the growth and solute accumulation of the halophyte Atriplex nummularia. Plant Soil **259**(1/2): 163–168

Raza A, Tabassum J, Fakhar AZ, Sharif R, Chen H, Zhang C, Ju L, Fotopoulos V, Siddique KHM, Singh RK, et al. (2022) Smart reprograming of plants against salinity stress using modern biotechnological tools. Crit Rev Biotechnol **15**(August): 1–28

Richter JA, Behr JH, Erban A, Kopka J, Zörb C (2019) Ion-dependent metabolic responses of Vicia faba L. To salt stress. Plant Cell Environ **42**(1): 295–309

Ródenas R, Martinez V, Nieves-cordones M, Rubio F (2019) High external K+ concentrations impair pi nutrition, induce the phosphate starvation response, and reduce arsenic toxicity in Arabidopsis plants. Int J Mol Sci **20**(9): 1–18

Shabala S (2017) Signalling by potassium: another second messenger to add to the list? J Exp Bot **68**(15): 4003–4007

Shabala S, Cuin TA (2008) Potassium transport and plant salt tolerance. Physiol Plant **133**(4): 651–669

Shi H, Ishitani M, Kim C, Zhu J-K (2000) The Arabidopsis thaliana salt tolerance gene SOS1 encodes a putative Na+/H+ antiporter. Proc Natl Acad Sci USA **97**(12): 6896–6901

Straub T, Ludewig U, Neuhäuser B (2017) The kinase CIPK23 inhibits ammonium transport in Arabidopsis thaliana. Plant Cell **29**(2): 409–422

Szyroki A, Ivashikina N, Dietrich P, Roelfsema MRG, Ache P, Reintanz B, Deeken R, Godde M, Felle H, Steinmeyer R, et al. (2001) KAT1 Is not essential for stomatal opening. Proc Natl Acad Sci U S A **98**(5): 2917–2921

Taji T, Ohsumi C, Iuchi S, Seki M, Kasuga M, Kobayashi M, Yamaguchi-Shinozaki K, Shinozaki K (2002) Important roles of drought- and cold-inducible genes for galactinol synthase in stress tolerance in Arabidopsis thaliana. Plant J **29**(4): 417–426

Tegeder M, Masclaux-Daubresse C (2018) Source and sink mechanisms of nitrogen transport and use. New Phytol **217**(1): 35–53

Thompson AR, Doelling JH, Suttangkakul A, Vierstra RD (2005) Autophagic nutrient recycling in Arabidopsis directed by the ATG8 and ATG12 conjugation pathways. Plant Physiol **138**(4): 2097–2110

Voelker C, Schmidt D, Mueller-roeber B, Czempinski K (2006) Members of the Arabidopsis AtTPK/KCO family form homomeric vacuolar channels in planta. Plant J **48**(2): 296–306

Wang X-P, Chen L-M, Liu W-X, Shen L-K, Wang F-L, Zhou Y, Zhang Z, Wu W-H, Wang Y (2016) AtKC1 and CIPK23 synergistically

modulate AKT1-mediated low-potassium stress responses in Arabidopsis. Plant Physiol **170**(4): 2264–2277

Wang G, DiTusa SF, Oh DH, Herrmann AD, Mendoza-Cozatl DG, O'Neill MA, Smith AP, Dassanayake M (2021) Cross species multi-omics reveals cell wall sequestration and elevated global transcription as mechanisms of boron tolerance in plants. New Phytol **230**(5): 1985–2000

Wang B, Lüttge U, Ratajczak R (2001) Effects of salt treatment and osmotic stress on V-ATPase and V-PPase in leaves of the halophyte Suaeda salsa. J Exp Bot **52**(365): 2355–2365

Wang G, Oh D, Dassanayake M (2020) GOMCL: a toolkit to cluster, evaluate, and extract non-redundant associations of gene ontology-based functions. BMC Bioinformatics **21**(1): 1–9

Wang Y, Wu W-H (2013) Potassium transport and signaling in higher plants. Annu Rev Plant Biol **64**(1): 451–476

Warren JK (2016) Potash resources: occurrences and controls. Evaporites. Springer International Publishing, Cham, pp 1081–1185

Yoshitake Y, Nakamura S, Shinozaki D, Izumi M (2021) RCB-mediated chlorophagy caused by oversupply of nitrogen suppresses phosphate-starvation stress in plants. Plant Physiol **185**(2): 318–330

Yuan L, Loqué D, Kojima S, Rauch S, Ishiyama K, Inoue E, Takahashi H, Von Wirén N (2007) The organization of high-affinity ammonium uptake in Arabidopsis roots depends on the spatial arrangement and biochemical properties of AMT1-type transporters. Plant Cell **19**(8): 2636–2652

Yuen CCY, Christopher DA (2013) The group IV-A cyclic nucleotide-gated channels, CNGC19 and CNGC20, localize to the vacuole membrane in Arabidopsis thaliana. AoB Plants **5**: 1–14

Zhang G-B, Yi H-Y, Gong J-M (2014) The *Arabidopsis* ethylene/jasmonic acid-NRT signaling module coordinates nitrate reallocation and the trade-off between growth and environmental adaptation. Plant Cell **26**(10): 3984-3998. http://dx.doi.org/10.1105/tpc.114.129296

Zhao W, Faust F, Schubert S (2020) Potassium is a potential toxicant for Arabidopsis thaliana under saline conditions. J Plant Nutr Soil Sci **183**(4): 455–467

Zhao S, Zhang M, Ma T-L, Wang Y (2016) Phosphorylation of ARF2 relieves its repression of transcription of the K+ transporter gene HAK5 in response to low potassium stress. Plant Cell **28**(12): 3005–3019

Zheng S, Pan T, Fan L, Qiu Q (2013) A novel AtKEA gene family, homolog of bacterial K+/H+ antiporters, plays potential roles in K + homeostasis and osmotic adjustment in Arabidopsis. PLoS One **8**-(11): e81463

Ziegler G, Terauchi A, Becker A, Armstrong P, Hudson K, Baxter I (2013) Ionomic screening of field-grown soybean identifies mutants with altered seed elemental composition. Plant Genome **6**(2): 0

Zioni A BEN, Vaadia Y, Lips SH (1971) Nitrate uptake by roots as regulated by nitrate reduction products of the shoot. Physiol Plant **24**(2): 288–290